

detecting breast disorders. Therefore, it has become very important to increase the rate of mammographic screening among the general public toward reducing the breast cancer mortality. However, it is also true that 7.2% of the malignant cases were associated with no mammographic abnormalities (3). In addition, the malignant ratio of 20, 30 and 40 years without mammographic abnormalities was statistically higher than the ratio of the other age groups (3). Ultrasonography (US) has been in general proposed to prove much more effective in the detection of breast cancer if the patient is young, has dense breast or their detected masses are small (4–6). Therefore, it has become very important to improve the quality of US diagnoses.

The effectiveness of ultrasound screening for women aged 40 years has been evaluated in detecting and reducing mortality of the breast cancer in Japan in order to complement this particular pitfall of mammography (7). This study named J-START (The Japan Strategic Anti-cancer Randomized Trial) evaluates the effectiveness of screening mammography with US breast cancer screening compared with mammography alone in 40 years, with a design to study 50 000 women with mammography and US and 50 000 controls with mammography only (7). The participants are scheduled to take a second-round screening with the same modality 2 years onwards (7). The primary endpoints are sensitivity and specificity, and the secondary endpoint as the rate of advanced breast cancer (7). Whether or not breast US screening is adopted in the future large-scale screening therefore largely depends on the results of this research. Considerable efforts will be required to successfully carry out this massive undertaking done in Japanese population.

Strict or rigorous conformity to high quality of interpretation of US finding among those involved in this screening is therefore mandatory for the very success of an US diagnosis in such a large scale. We previously examined the correlation between US findings and the corresponding histopathological features in breast disorders in our previous study (6). There have been relatively few reported studies on assessing US performance and its resolution without any mammographic abnormalities (8). Therefore, in this study, we evaluated US findings and the corresponding histopathological characteristics for breast cancer patients with Breast Imaging Reporting and Data System (BI-RADS) (9) category 1 mammogram.

PATIENTS AND METHODS

PATIENTS

We retrospectively reviewed the US findings and their corresponding histopathological features of 45 breast cancer patients with BI-RADS category 1 mammogram and 537 controls with mammographic abnormalities. The patients underwent needle biopsies or surgical resection at the Tohoku University Hospital from January 2006 to December 2010. We received informed consents from all the patients and the protocol for this study was approved by the Ethics Committee at Tohoku University Graduate School of Medicine.

IMAGING DEVICES AND BREAST TISSUE SPECIMENS

The US examinations were assessed by one of the experienced eight breast specialists in Tohoku University Hospital. The consensus meeting of US was held for 1 whole week in order to standardize the US examination among these eight doctors. In addition, two of them independently evaluated the US findings in a retrospective manner, without the knowledge of clinical and histopathological information of individual patients. All US evaluations were carried out using Aloka SSD 3500 and ProSound α 7 (Aloka Co., Tokyo, Japan) with a 10 MHz transducer.

We stained the corresponding tissue slides of the cases using hematoxylin–eosin (H&E) and immunohistochemistry for estrogen receptor (ER) and human epidermal growth factor receptor 2 (HER2). Surgical specimens had been fixed in 10% formaldehyde solution, cut into serial 5 mm-thick slices, embedded in paraffin, cut into 4 μ m-thick sections and placed on the glue-coated glass slides. We employed the avidin–streptavidin immunoperoxidase method using the clone 6F11 antibody (Ventana, Tucson, AZ, USA) in automated immunostainer (Benchmark System; Ventana). A standardized immunohistochemistry kit (HercepTest for Immunoenzymatic Staining; Dako, Copenhagen, Denmark) was used for HER2 staining. Histopathological slides were reviewed by two pathologists independently without the knowledge of clinical information. Olympus (Tokyo, Japan) BX50 and 20 \times objectives were used for the analyses.

IMAGING AND HISTOPATHOLOGICAL ANALYSES

Two or more hardcopy transverse and sagittal plane images of breast lesions were analyzed in this study. We recorded tumor shape, periphery, internal and lateral echo pattern, interruption of mammary borders and the distribution of low-echoic lesions, according to the BI-RADS sonographic classification (9) and the Japan Association of Breast and Thyroid Sonology (JABTS) breast sonographic classification (10). Tumor shape was tentatively classified into round, oval, lobular and irregular (9,10). Periphery was tentatively classified into circumscribed, obscured, indistinct and spiculated (9,10). Internal echo was classified into low and heterogeneity or high (9,10). Lateral echo was also classified into accentuation, no change and attenuation (9,10). Interruption of mammary borders was classified into interruption, indeterminate and no (9,10). Distribution of low-echoic lesions was classified into spotted and segmental (9,10) (Fig. 1).

Two of the experienced pathologists independently evaluated surgical pathology specimens, respectively. Histopathological evaluations were based on World Health Organization (WHO) histological classification of tumor of the breast (11) and Rosen's breast pathology (12). ER was determined by nuclear staining graded from 0 to 8 using the Allred score, and ER positivity was Grade 3 or more (13). With regard to HER2 evaluation, membranous staining was graded as the following: score 0–1+, 2+ and 3+ (14).

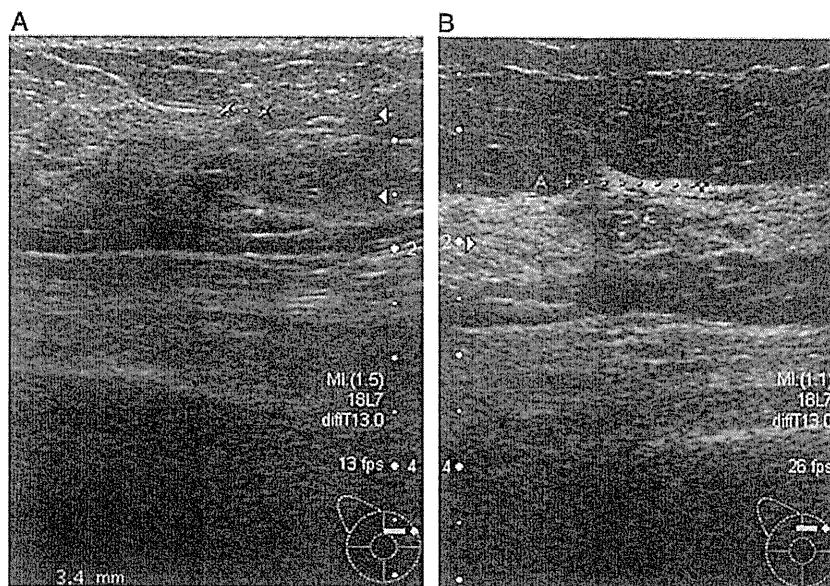


Figure 1. Representative illustrations of the distribution of low-echoic lesions. (A) Spotted and (B) segmental.

Scoring of 2+ was added fluorescence *in situ* hybridization (FISH) that was used to calculate the gene copy ratio of HER2-to-CEP17 (the PathVysion HER2 DNA Probe Kit; Abbott, Chicago, IL, USA). Positive is defined as either HER2:CEP17 signal ratio (FISH score) >2.2 (14). Histological grades and mitotic counts were assessed according to the criteria of Elston and Ellis (15). Van Nuys classifications were also assessed for ductal carcinoma *in situ* and invasive ductal carcinoma (IDC) with predominant intraductal components cases (16,17). We also identified the presence or absence of lymphovascular invasion according to the Rosen’s Breast Pathology (12).

At first, we examined the differences of the patients’ characteristics between these two groups including the distribution of age, menopausal status, past history of the benign proliferative disease, background of detection, clinical stage, breast density of mammography according to the BI-RADS lexicon (9) and surgical strategy as the breast-conserving ratio. We evaluated the US findings including mass shape, periphery, internal and posterior echo pattern, interruption of mammary borders and the distribution of low-echoic lesions and compared them with histopathological characteristics including histological classification, hormone receptor and HER2 status of IDC, tumor size confirmed by histopathology, histological grade, mitotic counts and lymphovascular invasion of BI-RADS category 1 mammograms. We then compared these findings with those of control group patients.

STATISTICAL ANALYSES

Statistical analyses were performed using StatMate III for Windows ver. 3.18 (ATMS, Tokyo, Japan). The results were considered significant at $P < 0.05$.

RESULTS

THE DETAILS OF BOTH BI-RADS 1 AND CONTROL GROUPS

Table 1 summarizes the difference in the patients’ characteristics including the distribution of age, menopausal status, past history of the benign proliferative disease, background of detection, clinical stage, breast density of mammography and surgical strategy. The median ages of the study group and the control group were 48 years (range, 32–84) and 56 years (range, 26–88), respectively ($P = 0.047$). There was a statistically significant higher ratio of Stages 0 and I, heterogeneously and extremely dense, and conserving surgery in the BI-RADS 1 group ($P < 0.001$, <0.001 and 0.002 , respectively). However, there was a statistically significant lower ratio of menopause and self-palpation in the BI-RADS 1 group ($P < 0.001$, respectively; Table 1).

Table 1. The details of patients

	BI-RADS 1	Control	P value	Odds ratio
Age	48 (32–84)	56 (26–88)	0.047	—
Menopausal ratio	37.8%	63.4%	<0.001	0.31
Benign proliferative disease	2.2%	9.5%	NS	2.34
Cause of detection (self-palpation ratio)	24.4%	59.4%	<0.001	0.22
Stage (Stages 0 and I)	93.3%	66.4%	<0.001	7.08
Heterogeneously and extremely dense ratio	91.1%	39.1%	<0.001	15.97
Surgical strategy (conserving ratio)	95.6%	74.6%	0.002	7.82

THE RATIOS OF MASS CASES AND THE TUMOR SIZE

Twenty-six out of the 45 were US mass cases in the BI-RADS 1 group and 370 out of the 490 were US mass cases in the control group. There was a statistically significant difference between the BI-RADS 1 and control groups ($P = 0.003$). The US tumor size of BI-RADS 1 and control groups was 12.1 mm (range, 3.2–24.9 mm) and 18.5 mm (range, 6.5–150 mm) with statistically significant differences ($P < 0.001$).

EVALUATION OF THE US CHARACTERISTICS

Figure 2 summarizes the results of the numbers and ratios of mass shape (Fig. 2A), periphery (Fig. 2B), internal echo pattern (Fig. 2C), lateral echo pattern (Fig. 2D) and interruption of mammary borders (Fig. 2E) of the BI-RADS 1 and control groups. There were statistically higher ratios of round mass shape ($P < 0.001$), no change of lateral echo pattern ($P = 0.028$) and no or indeterminate interruption of mammary borders ($P < 0.001$) in the BI-RADS 1 group. There were statistically lower ratios of spiculated periphery ($P = 0.021$), attenuation of lateral echo pattern ($P = 0.011$) and

interruption of mammary borders ($P < 0.001$) in the BI-RADS 1 group. Figure 3 summarizes the results of the numbers and ratios of distribution of low-echoic lesions. There were statistically higher ratios of spotted distribution and lower cases of segmental distribution in the BI-RADS 1 group than in the control group ($P = 0.012$).

EVALUATION OF THE CORRESPONDING HISTOPATHOLOGICAL CHARACTERISTICS

Figure 4 summarizes the results of the numbers and ratios of results classified by histological subtypes (Fig. 4A), hormone receptor and HER2 expression of IDC (Fig. 4B), tumor size of the invasive lesion as confirmed by the histopathological examination (Fig. 4C), histological grade (Fig. 4D), mitotic counts (Fig. 4E) and lymphovascular invasion (Fig. 4F). There was statistically higher ratios of triple-negative subtype, smaller tumor size and lower case of lymphovascular invasion in the BI-RADS 1 group ($P = 0.021$, $P < 0.001$ and $P = 0.012$, respectively) compared with the control group. In addition, a higher ratio of histological grade 3 was detected in the BI-RADS 1 group but this difference did not reach the statistical significance ($P = 0.094$).

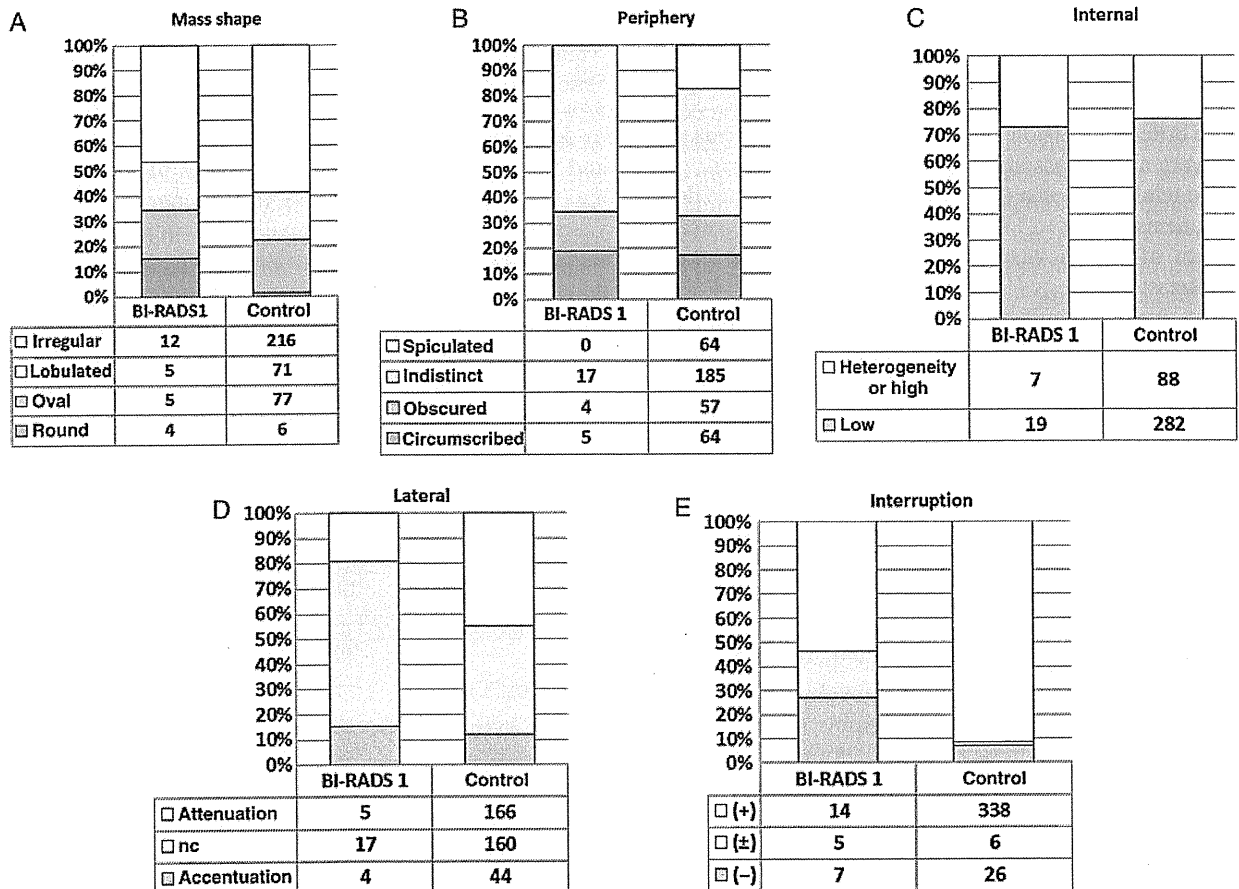


Figure 2. The US characteristics of BI-RADS category 1 and control groups. (A) Mass shape, (B) periphery, (C) internal echo pattern, (D) lateral echo pattern and (E) interruption of mammary borders.

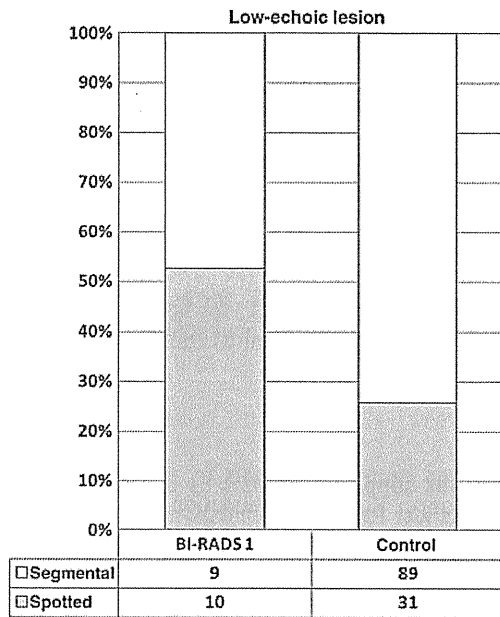


Figure 3. The distribution of low-echoic lesions of BI-RADS category 1 and control groups.

DISCUSSION

Mammography has been considered a gold standard for breast cancer screening system. However, US screening combined with mammography may have the potential to become one of the useful screening systems to decrease breast cancer mortality according to the results of the J-START trial (7). Therefore, strict or rigorous conformation to high quality of interpreting the US findings is required or mandatory for the future success of an US diagnosis especially at the level of mass screening. Our present study is the first study to focus upon incremental detection of breast cancer by US in asymptomatic women with mammography-negative breasts, and focused on the US findings and the corresponding histopathological characteristics of the cases with BI-RADS category 1 mammograms.

US detected cancers are in general smaller than those identified with mammography. Results of our present study demonstrated that the BI-RADS category 1 group was associated with a statistically higher ratio of low-echoic lesions than the control group. In addition, 52.6% of low-echoic lesions demonstrated spotted distribution in the BI-RADS 1 group, whereas 25.8% of low-echoic lesions spotted

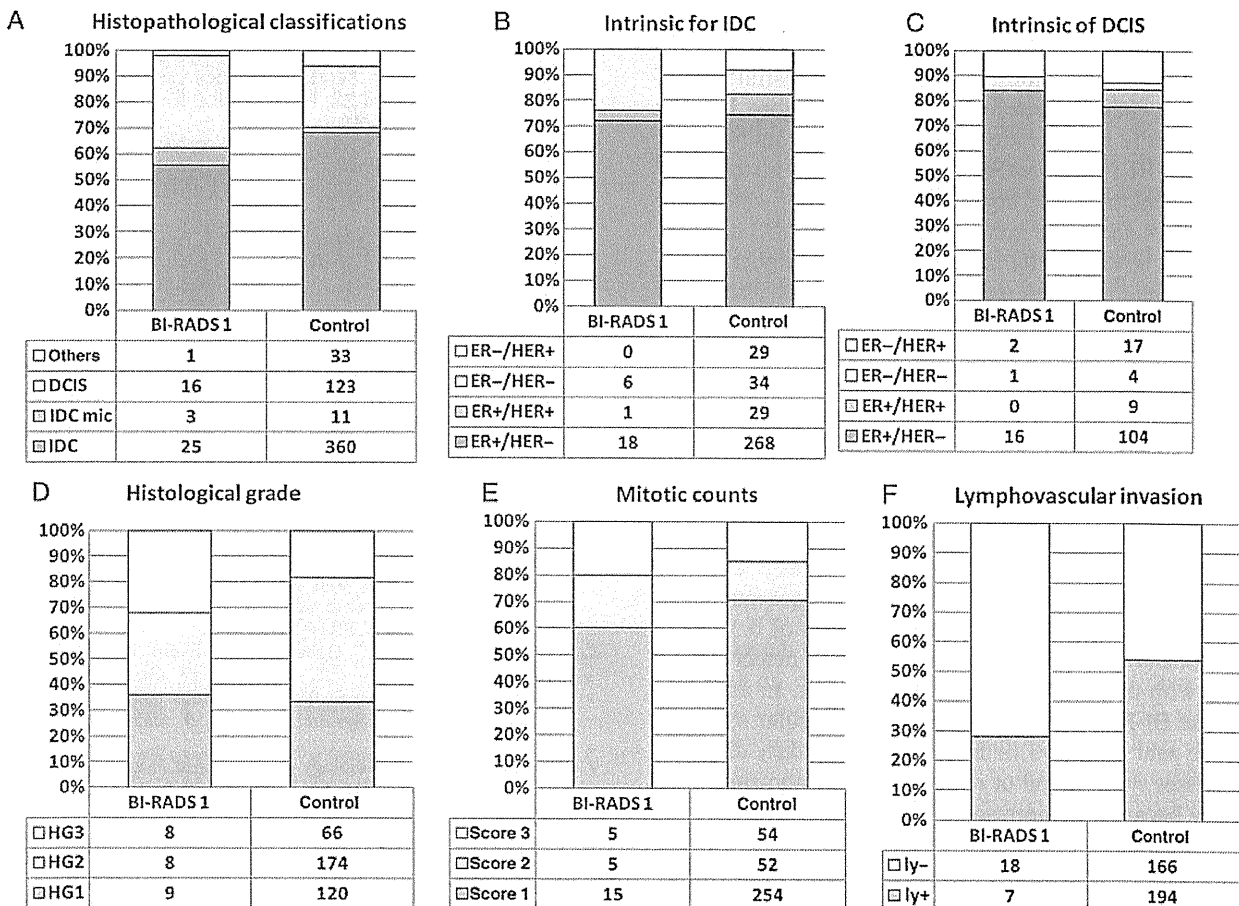


Figure 4. The histopathological characteristics of BI-RADS category 1 and control groups. (A) Histological classification, (B) hormone receptor and human epidermal growth factor receptor 2 expression of invasive ductal carcinoma, (C) tumor size of the invasive lesion, (D) histological grade, (E) mitotic counts and (F) lymphovascular invasion.

distribution in the control group. A low-echoic lesion with spotted distribution is therefore considered one of the predicting factors of malignancy in the BI-RADS category 1 group. In addition, the tumor size of the BI-RADS 1 group was smaller, and the detected masses were characterized by a higher ratio of round shape, non-spiculated periphery, non-interruption of mammary borders and non-attenuation in the BI-RADS category 1 group. These results could be mainly affected by mammographic breast density. In addition, results of our present study also demonstrated that there was a statistically higher ratio of heterogeneously and extremely dense breast in the BI-RADS 1 group and the tumors with well-collagenized stromal reaction were also detected as architectural distortion or spiculation in dense breast mammogram. Therefore, mammographic breast density was reasonably postulated to influence characteristics of breast cancers with BI-RADS category 1. Results of previous studies demonstrated that the most breast cancer cases of BI-RADS category 1 were relatively hypoechoic within a background of hyperechoic fibroglandular tissue, which may make the lesions more conspicuous and detectable (18). However, it is also true that previous studies have not evaluated the US findings of BI-RADS category 1 cases and this is the first study demonstrating the US findings such as mass shape and periphery of BI-RADS category 1 cases. In addition, this is the first reported study to demonstrate histopathological characteristics of BI-RADS category 1 cases. The statistically higher ratio of triple-negative subtype was detected in BI-RADS category 1 cases, and histological grade 3 tended to be also higher in the BI-RADS category 1 group. Results above did indicate that the BI-RADS category 1 group was histologically characterized by a higher malignant level than those with mammographic abnormalities, but it awaits further investigations for clarification.

Previous study also demonstrated that earlier detection of breast cancer resulted in a decrement in mortality, which parallels the reduction in size distribution of cancers depicted and closely parallels the reduction in rates of node-positive breast cancer (19). Screening US also appears to detect many breast cancer cases at a smaller size and earlier stage compared with mammographic screening. In addition, in women with mammography dense breast, US was reported to be able to detect a substantially larger number of cancers with a supplemental cancer detection of 0.3–0.5% by US alone (18). Therefore, it is important to detect the US findings with the localized low-echoic lesion. In addition, among the BI-RADS category 1 group, particular attention should be paid to the US findings such as solitary differentiated masses such as oval or round shape and non-spiculated periphery because the corresponding histopathological features of the cases associated with these US findings above include a much higher ratio of triple-negative subtype and/or histological grade 3. Therefore, early detection of such solitary masses with triple-negative subtype and/or high histological grade by US may possibly contribute to the eventual reduction in breast cancer mortality.

We evaluated US findings and the corresponding histopathological characteristics for BI-RADS category 1 mammograms and noted significant differences among these findings in this study. Evaluation of these US and histopathological characteristics may provide a more accurate US screening system for Japanese women.

Acknowledgement

We thank Yayoi Takahashi, MT, for her excellent technical assistance for immunohistochemical staining.

Funding

This work was supported in part by a Grant-in Aid from 'Kurokawa Cancer Research Foundation'.

Conflict of interest statement

None declared.

References

1. Sutela A, Vanninen R, Sudah M, Berg M, Kiviniemi V, Rummukainen J, et al. Surgical specimen can be replaced by core samples in assessment of ER, PR and HER-2 for invasive breast cancer. *Acta Oncol* 2008;47:38–46.
2. Kawai M, Kuriyama S, Suzuki A, Nishino Y, Ishida T, Ohnuki K, et al. Effect of screening mammography on breast cancer survival in comparison to other detection methods: a retrospective cohort study. *Cancer Sci* 2009;100:1479–84.
3. Tamaki K, Sasano H, Miyashita M, Ishida T, Amari M, Ohuchi N, et al. A new mammographic classification: as a potential predictor of breast disorders for Asian women. 12th International St Gallen Breast Cancer Conference, St Gallen, Switzerland, 2011, SG-BCC2011-1204.
4. Osako T, Takahashi K, Iwase T, Iijima K, Miyagi Y, Nishimura S, et al. Diagnostic ultrasonography and mammography for invasive and noninvasive breast cancer in women aged 30–39 years. *Breast Cancer* 2007;14:229–33.
5. Crystal P, Strano SD, Shcharynski S, Koretz MJ. Using sonography to screen women with mammographically dense breasts. *Am J Roentgenol* 2003;181:177–82.
6. Tamaki K, Sasano H, Ishida T, Ishida K, Miyashita M, Takeda M, et al. The correlation between ultrasonographic findings and pathologic features in breast disorders. *Jpn J Clin Oncol* 2010;40:905–12.
7. Ohuchi N, Ishida T, Kawai M, Narikawa Y, Yamamoto S, Sobue T. Randomized controlled trial on effectiveness of ultrasonography screening for breast cancer in women aged 40–49 (J-START): research design. *Jpn J Clin Oncol* 2011;41:275–7.
8. Zanello PA, Robim AFC, Goncalves de Oliveira TM, Elias Junior J, Andrade JM, Monteiro CR, et al. Breast ultrasound diagnostic performance and outcomes for mass lesions using Breast Imaging Reporting and Data System category 0 mammogram. *Clinics* 2011;66:443–8.
9. American College of Radiology (ACR). *Breast Imaging Reporting and Data System (BI-RADS™)*. 4th edn. Reston, VA: American College of Radiology 2003.
10. Japan Association of Breast and Thyroid Sonography. *Guideline for Breast Ultrasound-Management and Diagnosis*. 2nd edn. Tokyo: Japanese 2008.
11. Tavassoli FA, Devilee P. *World Health Organization Classification of Tumors. Tumor of the Breast and Females Genital Organs*. Lyon: IARC Press 2003.
12. Rosen PP. *Rosen's Breast Pathology*. 3rd edn. Philadelphia, PA: Lippincott Williams & Wilkins 2009.

13. Allred DC, Harvey JM, Berardo M, Clark GM. Prognostic and predictive factors in breast cancer by immunohistochemical analysis. *Mod Pathol* 1998;11:155–68.
14. Wolff AC, Hammond ME, Schwartz JN, Hagerty KL, Allred DC, Cote RJ, et al. American society of clinical oncology/college of American pathologists guideline recommendations for human epidermal growth factor receptor 2 testing in breast cancer. *J Clin Oncol* 2007;25:118–45.
15. Elston CW, Ellis IO. Pathological prognostic factors in breast cancer. I. The value of histopathological grade in breast cancer: experience from a large study with long-term follow-up. *Histopathology* 1991;19:403–10.
16. Silverstein MJ. Prognostic classification of breast ductal carcinoma in situ. *Lancet* 1995;345:1154–7.
17. Tamaki K, Moriya T, Sato Y, Ishida T, Maruo Y, Yoshinaga K, et al. Vasohibin-1 in human breast carcinoma: a potential negative feedback regulator of angiogenesis. *Cancer Sci* 2009;100:88–94.
18. Youk JH, Kim EK. Supplementary screening sonography in mammographically dense breast: pros and cons. *Korean J Radiol* 2010;11:589–93.
19. Berg WA. Beyond standard mammographic screening: mammography at age extremes, ultrasound, and MR imaging. *Radiol Clin North Am* 2007;45:895–906.

Nucleobindin 2 in human breast carcinoma as a potent prognostic factor

Shiho Suzuki,¹ Kiyoshi Takagi,^{1,5} Yasuhiro Miki,² Yoshiaki Onodera,² Jun-ichi Akahira,² Akiko Ebata,^{2,3} Takanori Ishida,³ Mika Watanabe,⁴ Hironobu Sasano^{2,4} and Takashi Suzuki¹

Departments of ¹Pathology and Histotechnology, ²Anatomic Pathology, ³Surgical Oncology, Tohoku University Graduate School of Medicine, Sendai; ⁴Department of Pathology, Tohoku University Hospital, Sendai, Japan

(Received June 20, 2011/Revised September 15, 2011/Accepted September 27, 2011/Accepted manuscript online October 11, 2011/Article first published online November 17, 2011)

It is well-known that estrogens immensely contribute to the progression of human breast carcinoma, but their detailed molecular mechanisms remain largely unclear. In this study, we identified nucleobindin 2 (*NUCB2*) as a gene associated with recurrence based on microarray data of estrogen receptor (ER)-positive breast carcinoma cases ($n = 10$), and subsequent *in vitro* study showed that *NUCB2* expression was upregulated by estradiol in ER-positive MCF-7 cells. However, *NUCB2* has not yet been examined in breast carcinoma, and its significance remains unknown. Therefore, we further examined the biological functions of *NUCB2* in breast carcinoma using immunohistochemistry and *in vitro* studies. *NUCB2* immunoreactivity was detected in carcinoma cells in 77 of 161 (48%) breast cancer cases, and positively associated with lymph node metastasis and ER status of the patients. In addition, *NUCB2* status was significantly associated with an increased risk of recurrence and adverse clinical outcome of the patients using both univariate and multivariate analyses. Results of siRNA transfection experiments showed that *NUCB2* significantly increased cell proliferation, and migration and invasion properties in both MCF-7 and ER-negative SK-BR-3 cells. These results suggest that *NUCB2* is upregulated by estrogens and plays an important role, especially in the process of metastasis, in breast carcinomas. *NUCB2* status is considered a potent prognostic factor in human breast cancer. (*Cancer Sci* 2012; 103: 136–143)

Breast cancer is one of the most common malignancies in women. Estrogens play an important role in the progression of breast cancer through an interaction with ER, and ER is positive in approximately two-thirds of breast carcinoma cases. The great majority of ER-positive breast carcinomas respond to endocrine therapy such as tamoxifen and aromatase inhibitors, but it is also true that some of these carcinomas acquire clinical resistance to endocrine therapy.^(1,2)

Estrogen receptor activates the transcription of various target genes in a ligand-dependent manner by binding EREs located in the promoter region. Various estrogenic functions are characterized by the expression patterns of these genes, which make it extremely important to examine the expression and roles of estrogen-responsive genes to obtain a better understanding of estrogenic actions such as progression, recurrence, and resistance to endocrine therapy.⁽³⁾ Various estrogen-responsive genes have been identified in breast carcinoma,^(4,5) but their detailed clinical significance and/or function remain unclear in a great majority of these genes. Therefore, in this study, we first studied the expression profiles of genes containing ERE in ER-positive breast carcinoma tissues based on microarray data, and identified *NUCB2* as a possible gene associated with recurrence in these patients.

Nucleobindin 2 has a characteristic constitution of functional domains, such as a signal peptide, a Leu/Ile rich region, two Ca²⁺ binding EF-hand domains separated by an acidic amino acid-rich region, and a leucine zipper,^(6,7) and has a wide variety of basic cellular functions.^(8–10) However, to the best of our

knowledge, *NUCB2* has not yet been studied in breast carcinoma. Therefore, we examined *NUCB2* in breast carcinoma using immunohistochemistry and *in vitro* studies to explore its clinical and biological significance.

Materials and Methods

Patients and tissues. Two sets of tissue specimens were evaluated in this study. As a first set, 10 specimens of ER-positive breast carcinoma were obtained from women (age range, 48–74 years) who underwent surgical treatment in 2001 or 2002 in the Department of Surgery, Tohoku University Hospital (Sendai, Japan). All patients received tamoxifen therapy after surgery. The status of recurrence was evaluated whether the first locoregional recurrence or distant metastasis was detected within the follow-up time after surgery (mean, 80 months; range, 37–204 months) or not. These specimens were stored at -80°C for microarray analysis.

As a second set, 161 specimens of invasive ductal carcinoma of human breast were obtained from women who underwent surgical treatment between 1984 and 1997 in the Department of Surgery, Tohoku University Hospital. The patients did not receive chemotherapy, irradiation, or hormonal therapy before the surgery. Review of the charts revealed that 125 patients received adjuvant chemotherapy, 66 patients received tamoxifen therapy, and 12 patients received radiation therapy following surgery. The clinical outcome of the patients was evaluated by disease-free and breast cancer-specific survival. The mean age was 54 years (range, 22–81 years), and the mean follow-up time was 103 months (range, 3–157 months). Mitotic score and histological grade were evaluated according to a previous report.⁽¹¹⁾ All the specimens were fixed in 10% formalin and embedded in paraffin wax.

Research protocols for this study were approved by the Ethics Committee at Tohoku University School of Medicine (Sendai, Japan).

Laser capture microdissection/microarray analysis. Gene expression profiles of breast carcinoma cells in the first set ($n = 10$) were examined using microarray analysis. Gene expression profile data was assembled previously.^(12,13) Briefly, approximately 5000 breast carcinoma cells were laser transferred from the frozen section, and total RNA was subsequently extracted. In this study, we focused on the expression of 519 genes identified to have a functional ERE by Bourdeau *et al.*⁽¹⁴⁾

Immunohistochemistry. Rabbit polyclonal antibody for *NUCB2* and *HER2* (A0485) were purchased from Aviva Systems Biology (San Diego, CA, USA) and Dako (Carpinteria, CA, USA), respectively. Monoclonal antibodies for ER (ER1D5), PR (MAB429), and Ki-67 (MIB1) were purchased

⁵To whom correspondence should be addressed.
E-mail: k-takagi@med.tohoku.ac.jp

from Immunotech (Marseille, France), Chemicon (Temecula, CA, USA), and Dako, respectively.

A Histofine Kit (Nichirei, Tokyo, Japan), which incorporates the streptavidin–biotin amplification method, was used. The antigen–antibody complex was visualized with 3,3'-diaminobenzidine and counterstained with hematoxylin. Human tissue of the stomach was used as a positive control for NUCB2 antibody,⁽¹⁵⁾ and normal rabbit IgG was used instead of the primary antibody, as a negative control of NUCB2 immunostaining.

NUCB2 immunoreactivity was detected in the cytoplasm of breast carcinoma cells, and the cases that had more than 10% of positive carcinoma cells were considered positive for NUCB2 status. Immunoreactivity for ER, PR, and Ki-67 was detected in the nucleus, and the immunoreactivity was evaluated in more than 1000 carcinoma cells for each case. The percentage of immunoreactivity, that is, the LI, was determined. Cases with an ER LI or PR LI of more than 10% were considered ER- or PR-positive breast carcinoma, respectively, according to a previous report.⁽¹⁶⁾

Immunoblotting. The protein of MCF-7 cells was extracted using M-PER Mammalian Protein Extraction Reagent (Pierce Biotechnology, Rockford, IL, USA) with Halt Protease Inhibitor Cocktail (Pierce Biotechnology). Twenty micrograms of the protein (whole cell extracts) was subjected to SDS-PAGE (10% acrylamide gel). Following SDS-PAGE, proteins were transferred onto Hybond-P PVDF membrane (GE Healthcare, Chalfont St Giles, UK). Primary antibody was the same anti-NUCB2 antibody used in the immunohistochemistry (Aviva Systems Biology). Antibody–protein complexes on the blots were detected using ECL Plus Western blotting detection reagents (GE Healthcare), and the protein bands were visualized with a LAS-1000 image analyzer (Fuji Photo Film, Tokyo, Japan).

Real-time PCR. Total RNA was extracted using TRIzol reagent (Invitrogen, Carlsbad, CA, USA), and cDNA was synthesized using a QuantiTect reverse transcription Kit (Qiagen, Hilden, Germany). Real-time PCR was carried out using the LightCycler System and FastStart DNA Master SYBR Green I (Roche Diagnostics, Mannheim, Germany). The primer sequences of NUCB2 and the ribosomal protein L13A (RPL13A) were: NUCB2, 5'-AAAGAAGAGCTACAACGTCA-3' (forward) and 5'-GTGGCTCAAACCTCAATTC-3' (reverse); and RPL13A, 5'-CCTGGAGGAGAAGAGGAAA-GAGA-3' (forward) and 5'-TTGAGGACCTCTGTATTGTCAA-3' (reverse). The NUCB2 mRNA level was calculated as the ratio of the RPL13A mRNA level.

Small interfering RNA transfection. Small interfering RNA for NUCB2 was purchased from Ambion (Austin, TX, USA). The target sequences of siRNA against NUCB2 were as follows: si1, 5'-UAUCUUCGCACUUUCCACAGGGUGA-3' (sense) and 5'-UCACCCUGUGGAAAGUGCGAAGUA-3' (anti-sense); and si2, 5'-UUGAUUAGCAUAUCUAAAUCUGUGG-3' (sense) and 5'-CCACAGAUUUAGAUUGCUAAUCA-3' (anti-sense). In addition, medium GC duplex #2 (Invitrogen) was also used as a negative control (siC). The siRNA was transfected using HiperFect transfection reagent (Qiagen).

Cell proliferation, migration, and invasion assays. MCF-7 and SK-BR-3 cells were transfected with NUCB2-specific siRNA or control siRNA in a 96-well culture plate. Three days after transfection, the cell number was evaluated using a Cell Counting Kit-8 (Dojindo, Kumamoto, Japan).

The cell migration assay was carried out using a 24-well plate and Chemotaxicell (8 μ m pore size; Kurabo, Osaka, Japan) according to a previous report.⁽¹⁷⁾ MCF-7 and SK-BR-3 cells were plated at the upper chamber, and the cells on the upper surface of the membrane were removed after incubation for 72 h. The migration ability was evaluated as an average number of cells in five middle power fields ($\times 200$) randomly selected on the lower surface of the membrane.

The cell invasion assay was carried out using a modified migration assay. The upper surface of the membrane of a Chemotaxicell was coated with 80 mg/cm² of Matrigel basement membrane matrix (BD Biosciences, Heidelberg, Germany), and the invasion ability was evaluated as the total number of cells on the lower surface of the membrane.

Results

Comparison of gene expression profiles between recurrent and non-recurrent groups of breast carcinoma patients. The microarray data used in this study are available through the National Center for Biotechnology Information Gene Expression Omnibus database (accession GSE11965, <http://www.ncbi.nlm.nih.gov/geo>). In this analysis, when the expression ratio of a gene in the recurrence group compared to that in the non-recurrence group was more than 2.0 or <0.5, we determined that the gene was predominantly expressed in the recurrence or non-recurrence group, respectively.

As shown in Figure 1(A), of the 519 genes examined, the number of genes predominantly expressed in the recurrence group (group A) was 17 (3%); the number of genes predominantly expressed in the non-recurrence group (group B) was 35 (7%). A great majority of the genes (467 genes; 90%) had a similar expression level in each of the two groups (ratio 0.5–2.0) (group C). The lists of genes classified in group A and group B are summarized in the right panel of Figure 1(A), and in Table S1. When we carried out gene ontology enrichment analysis between groups A and B (<http://cbl-gorilla.cs.technion.ac.il/>), no significant enriched gene ontology term was detected. Among the genes in Group A, NUCB2 showed the highest ratio (4.9) and expression level, indicating its possible involvement in the recurrence in ER-positive breast carcinoma patients after surgery.

The NUCB2 gene contains functional ERE in the promoter region⁽¹⁴⁾ but the regulation of NUCB2 expression by estradiol has not been investigated in breast carcinoma cells. As shown in Figure 1(B), NUCB2 mRNA expression was significantly increased by estradiol treatment for 3 days in MCF-7 cells. However, the NUCB2 mRNA expression level was significantly lower ($P < 0.05$, and 0.3-fold) than the basal level, when the cells were treated together with estradiol (10 nM) and a potent ER antagonist ICI 182780 (1 μ M). When MCF-7 cells were treated with estradiol (10 nM) and anti-estrogen tamoxifen (10 μ M), the NUCB2 mRNA level was not significantly changed compared to the basal level ($P = 0.10$, and 1.5-fold). Estradiol (10 nM) time-dependently induced NUCB2 mRNA expression in MCF-7 cells (Fig. 1C).

NUCB2 immunolocalization in human breast carcinoma. As shown in Figure 2(A), immunoblot analysis for NUCB2 revealed a specific band (approximately 43 kDa) in MCF-7 cells, which confirmed the specificity of the anti-NUCB2 antibody used in this study.⁽¹⁸⁾ In the immunohistochemistry, NUCB2 immunoreactivity was detected in the cytoplasm of breast carcinoma cells (Fig. 2B). NUCB2 immunoreactivity was weakly and focally detected in the epithelial cells of morphologically normal glands (Fig. 2C), but it was negative in the stroma. In the positive control, NUCB2 was mainly positive in the epithelium of the fundic glands in the stomach (Fig. 2D), as reported previously,⁽¹⁵⁾ whereas no significant immunoreactivity was detected in the same areas of the negative control section (Fig. 2E).

Associations between NUCB2 immunohistochemical status and various clinicopathological parameters in breast carcinomas are summarized in Table 1. Of 161 cases of breast carcinoma examined in this study, 77 (48%) were NUCB2-positive. NUCB2 status was significantly associated with lymph node metastasis ($P = 0.004$) and ER status ($P = 0.002$) of the patients, whereas no significant association was detected in patients' age, menopausal status, clinical stage, tumor size,

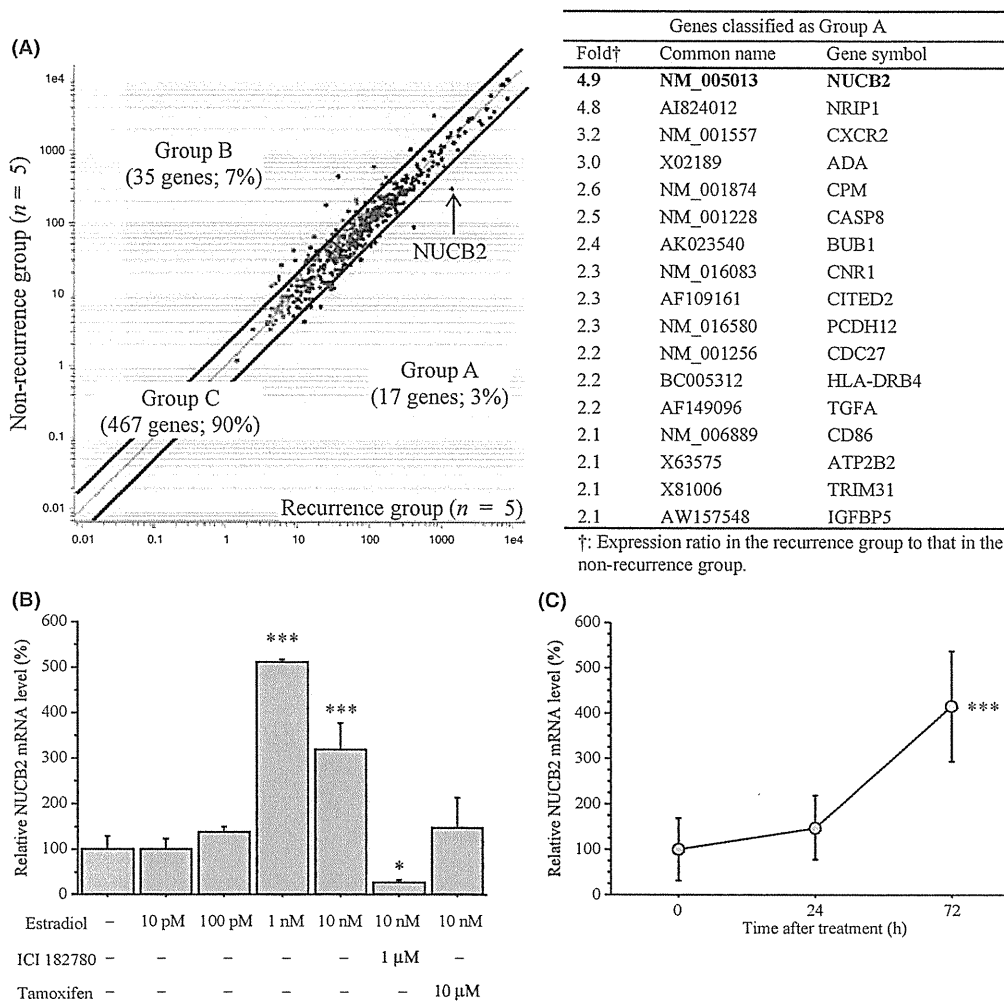


Fig. 1. Nucleobindin 2 (*NUCB2*) as an estrogen-induced gene associated with breast carcinoma. (A) Scatter plot analysis of microarray data for 519 genes containing functional estrogen-responsive element in breast carcinomas comparing the recurrence and non-recurrence group ($n = 5$ in each group). Genes with an expression ratio, recurrence group to non-recurrence group, of more than 2.0 or <0.5 are located outside the diagonal line, and classified as group A or group B, respectively. Genes with a ratio between 2.0 and 0.5 were classified as group C. *NUCB2* showed the highest ratio in these genes (arrow). The right panel summarizes the gene list of group A. (B,C) Effects of estradiol on *NUCB2* mRNA expression. MCF-7 cells were treated with indicated concentrations of estradiol with or without (–) ICI 182780 or tamoxifen for 3 days (B) or treated with estradiol (10 nM) for the indicated period (C). The relative *NUCB2* mRNA level summarized as a ratio (%) compared with the basal level (non-treatment). Data are presented as the mean \pm SD ($n = 3$). * $P < 0.05$ and *** $P < 0.001$ versus non-treatment (left bar) (B) or 0 h (left plot) (C).

histological grade, mitotic score, PR status, *HER2* status, or Ki-67 LI. The positive association between *NUCB2* status and lymph node metastasis was significant regardless of the ER status of these cases ($P = 0.02$) (Table S2). *NUCB2* status was positively associated with Ki-67 LI in the ER-positive group ($P = 0.02$), and was positively correlated with tumor size in ER-negative cases ($P = 0.03$).

When immunohistochemistry was carried out in ductal carcinoma *in situ*, *NUCB2* immunoreactivity was detected in the carcinoma cells (Fig. 2F) in 7 (32%) of 22 cases. The *NUCB2* positivity was 1.5-fold higher in invasive carcinoma (48%) than non-invasive carcinoma (32%), although it did not reach a level of significance ($P = 0.15$).

Association between *NUCB2* status and clinical outcome. In order to thoroughly examine the association between *NUCB2* status and patient prognosis, we excluded stage IV cases and used stage I–III breast carcinoma patients ($n = 141$) in the following analyses. As shown in Figure 3(A), *NUCB2* status

was significantly associated with an increased incidence of recurrence ($P = 0.003$), and the multivariate analysis revealed that lymph node metastasis ($P = 0.01$), ER status ($P = 0.002$), and *NUCB2* status ($P = 0.001$) were independent prognostic factors for disease-free survival with relative risks over 1.0 (Table 2).

A breast cancer-specific survival curve of the patients is summarized in Figure 3(B); a significant correlation ($P = 0.0002$) was detected between *NUCB2* status and adverse clinical outcome in the 141 breast carcinoma patients examined. In the univariate analysis (Table 2), lymph node metastasis ($P = 0.0004$), *NUCB2* status ($P = 0.002$), ER status ($P = 0.003$), histological grade ($P = 0.01$), *HER2* status ($P = 0.01$), and tumor size ($P = 0.02$) were all indicated as significant prognostic variables for breast cancer-specific survival. A following multivariate analysis showed that only *NUCB2* status ($P = 0.0004$) and ER status ($P = 0.01$) were independent prognostic factors with a relative risk over 1.0, whereas lymph node metastasis

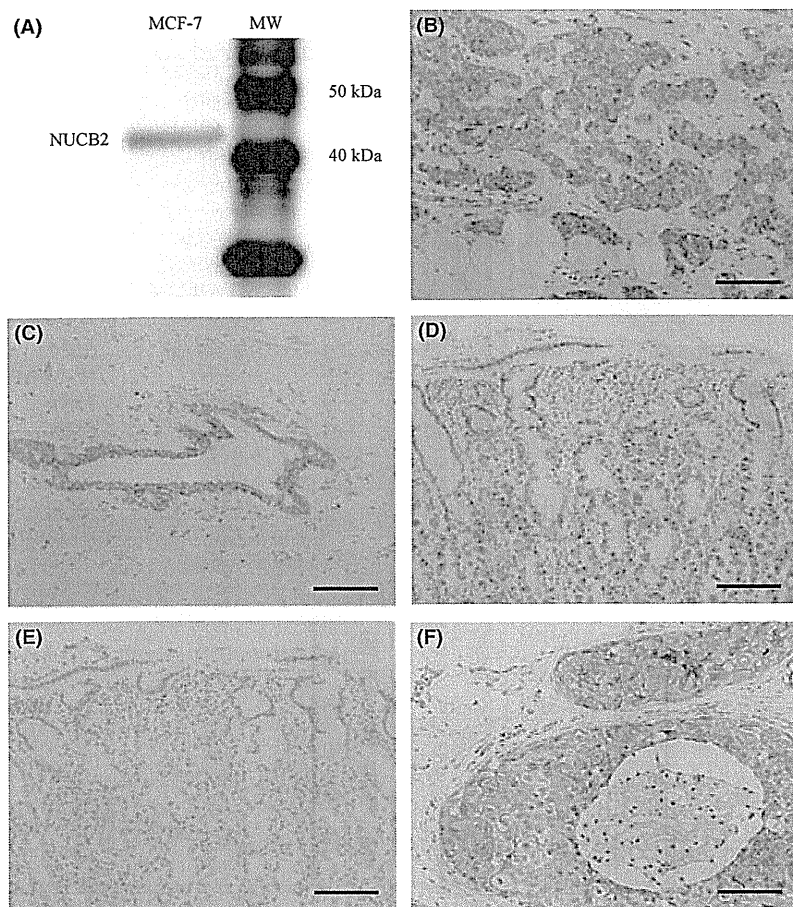


Fig. 2. Immunohistochemistry for nucleobindin 2 (*NUCB2*) in breast carcinoma. (A) Immunoblotting for *NUCB2* in MCF-7 cells. MW, molecular weight. (B) *NUCB2* immunoreactivity was detected in the carcinoma cells of invasive ductal carcinoma. (C) *NUCB2* immunoreactivity was weakly and focally detected in morphologically normal mammary glands. (D) Positive control section of *NUCB2* immunohistochemistry (gastric mucosa). (E) Negative control section of *NUCB2* immunohistochemistry (same area as Fig. 2D). (F) *NUCB2* immunoreactivity was detected in the carcinoma cells of ductal carcinoma *in situ*. Bar = 100 μm .

($P = 0.22$), histological grade ($P = 0.28$), *HER2* status ($P = 0.60$), and tumor size ($P = 0.07$) were not significant.

A similar association between *NUCB2* and worse prognosis was detected regardless of the Ki-67 status ($P = 0.03$ in cases with Ki-67 LI $\geq 10\%$ and $P = 0.04$ in cases with Ki-67 $< 10\%$ for disease-free survival [Fig. 3C]; $P = 0.004$ in cases with Ki-67 LI $\geq 10\%$ and P -value not available cases with Ki-67 $< 10\%$ because no patient died in the *NUCB2*-negative group for breast cancer-specific survival). When the 66 *NUCB2*-positive cases were further categorized into two groups according to immunointensity (++, strongly positive [$n = 16$]; +, modestly positive [$n = 50$]), no significant difference was detected between these two groups ($P = 0.60$ for disease-free survival [Fig. 3D], and $P = 0.49$ for breast cancer-specific survival).

Forty patients with stage I–III disease received tamoxifen therapy following surgery as an adjuvant treatment, and these cases were all positive for ER. *NUCB2* status was also markedly associated with an increased risk of recurrence (Fig. 3E) and worse prognosis (data not shown) in the patients who received tamoxifen therapy, although P -values were not available because no patient had recurrent disease or died in the group of *NUCB2*-negative cases. Significant association between *NUCB2* status and patients' clinical outcome was also detected in the 113 patients who received adjuvant chemotherapy ($P = 0.03$ for disease-free and $P = 0.002$ for breast cancer-specific survival),

38 ER-negative cases ($P = 0.0001$ for disease-free and $P < 0.0001$ for breast cancer-specific survival), or 24 cases with ER LI $< 1\%$ ($P = 0.001$ for disease-free [Fig. 3F] and $P = 0.0004$ for breast cancer-specific survival).

Effects of *NUCB2* expression on cell proliferation and invasion in breast carcinoma cells. The results of our study suggest that *NUCB2* is associated with worse prognosis of breast carcinoma patients regardless of their ER status, although *NUCB2* expression is upregulated by estrogen. In order to further examine the biological functions of *NUCB2* in human breast carcinoma, we transfected specific siRNA for *NUCB2* both in ER-positive MCF-7 and ER-negative SK-BR-3 breast carcinoma cells. The *NUCB2* mRNA expression level was markedly decreased in these cells transfected with specific *NUCB2* siRNA (si1 or si2) at 3 days after transfection compared to cells transfected with control siRNA (siC). The ratio of *NUCB2* mRNA level compared to that in the control siRNA was: MCF-7, 5% (si1) and 8% (si2); and SK-BR-3, 11% (si1) and 12% (si2).

As shown in Figure 4(A), the number of cells was significantly lower in MCF-7 cells transfected with *NUCB2* siRNA ($P < 0.001$ and 0.52-fold in si1, and $P < 0.001$ and 0.64-fold in si2) than in control cells transfected with siC 3 days after the transfection. A similar association was also detected in SK-BR-3 cells under the same conditions ($P < 0.001$ and 0.75-fold in si1, and $P < 0.001$ and 0.81-fold in si2). Figure 4(B) shows the

Table 1. Association between nucleobindin 2 (NUCB2) immunohistochemical status and clinicopathological parameters in 161 breast carcinomas

	NUCB2 status		P-value
	Positive (n = 77)	Negative (n = 84)	
Age† (years)	53.9 ± 1.4	54.4 ± 1.2	0.770
Menopausal status (%)			0.860
Premenopausal	31 (19)	35 (22)	
Postmenopausal	46 (29)	49 (30)	
Stage (%)			0.730
I	18 (11)	24 (15)	
II	38 (24)	43 (27)	
III	10 (6)	8 (5)	
IV	11 (7)	9 (6)	
Tumor size† (cm)	3.4 ± 0.4	3.4 ± 0.4	0.990
Lymph node metastasis (%)			0.004
Positive	41 (25)	26 (16)	
Negative	36 (22)	58 (36)	
Histological grade (%)			0.930
1 (well)	20 (12)	24 (15)	
2 (moderate)	30 (19)	31 (19)	
3 (poor)	27 (17)	29 (18)	
Mitotic score (%)			0.570
1 (low)	33 (20)	43 (27)	
2 (moderate)	22 (14)	21 (13)	
3 (high)	22 (14)	20 (12)	
ER status (%)			0.002
Positive	65 (40)	53 (33)	
Negative	12 (7)	31 (19)	
PR status (%)			0.150
Positive	55 (34)	51 (32)	
Negative	22 (14)	33 (20)	
HER2 status (%)			0.990
Positive	22 (14)	24 (15)	
Negative	55 (34)	60 (37)	
Ki-67 LI† (%)	23.6 ± 1.8	21.1 ± 2.1	0.380

†Data are presented as the mean ± SEM. All other values represent the number of cases and percentage. ER, estrogen receptor; LI, labeling index; PR, progesterone receptor. P-values <0.05 were considered significant, indicated in bold.

results of the migration assay. The number of migrated cells was significantly lower in both MCF-7 cells ($P < 0.001$ and 0.11-fold in si1, and $P < 0.001$ and 0.43-fold in si2) and SK-BR-3 cells ($P < 0.001$ and 0.36-fold in si1, and $P < 0.001$ and 0.31-fold in si2) transfected with *NUCB2* siRNA than in those transfected with control siRNA at 1 day (MCF-7) or 2 days (SK-BR-3) after the transfection. Moreover, the number of invaded cells was also significantly lower in the cells transfected with *NUCB2* siRNA (MCF-7, $P < 0.05$ and 0.21-fold in si1 and $P < 0.05$ and 0.29-fold in si2; SK-BR-3, $P < 0.01$ and 0.66-fold in si1 and $P < 0.001$ and 0.47-fold in si2) (Fig. 4C,D).

Discussion

Gene expression profiling is an important method to predict the likelihood of recurrence of disease in breast cancer patients,⁽¹⁹⁾ in addition to conventional clinical and histopathological examination. A multigene classifier associated with recurrence has been proposed for breast carcinoma patients by several research groups,^(19–21) and molecular-based diagnostic systems have been developed, such as MammaPrint⁽²²⁾ and Oncotype DX,⁽²³⁾ as well as the genomic grade index.⁽²⁴⁾ However, the selected genes vary markedly between these diagnostic systems, which may be partly due to the fact that they use different platforms for the analysis of gene expression. In addition, the biological

functions have remained largely unknown in a great majority of these genes. In our present study, the results of microarray analysis revealed 17 genes that are potentially associated with recurrence in ER-positive breast carcinoma patients (group A in Fig. 1A). Among these, *IGFBP5* (insulin-like growth factor-binding protein 5) was reported to play an important role in breast carcinoma metastasis,^(25,26) and is included in MammaPrint. In addition, *TGFA* (transforming growth factor α), a member of the epidermal growth factor family, is well-known to be involved in cellular proliferation and carcinogenesis.⁽²⁷⁾ The kinetochore-bound protein kinase *BUB1* (budding uninhibited by benzimidazoles 1) is a possible link to tumorigenesis.⁽²⁸⁾ *NUCB2* showed the highest expression ratio in this study, but this gene has not been listed in any multigene classifiers predicting breast carcinoma recurrence, nor has it been examined in breast carcinoma, to the best of our knowledge.

In this study, we first showed that *NUCB2* immunoreactivity was detected in 48% of breast carcinoma cases, although levels were almost negligible in morphologically normal mammary glands. *NUCB2* is known to mainly express in key hypothalamic nuclei with proven roles in energy homeostasis.⁽⁹⁾ Moreover, recent investigations have indicated that *NUCB2* is also expressed in various human peripheral tissues, including the stomach, pancreas, reproductive organs, and adipose tissues, with relevant metabolic functions, suggesting that *NUCB2* signaling might participate in adaptative responses and in the control of body functions gated by the state of energy reserves.⁽²⁹⁾ However, *NUCB2* expression in carcinoma has only been examined in the stomach; Kalnina *et al.*⁽¹⁵⁾ reported that *NUCB2* immunoreactivity was not detected in carcinoma cells in 15 gastric carcinoma cases examined. The relatively wide distribution of *NUCB2* immunoreactivity in our present study suggests that *NUCB2* plays an important role in human breast carcinoma.

Bourdeau *et al.*⁽¹⁴⁾ evaluated genome-wide identification of EREs in humans, and identified a functional ERE element at 8257 bp from the most upstream mRNA 5'-end of the *NUCB2* gene. In our present study, *NUCB2* immunohistochemical status was positively associated with ER status in breast carcinoma tissue, and *NUCB2* mRNA was significantly upregulated by estradiol in MCF-7 cells through ER. Therefore, *NUCB2* is considered one of the estrogen-induced genes in breast carcinoma cells. Results of our present study also indicated the presence of *NUCB2* in 12 of 43 (28%) ER-negative breast carcinoma cases; it might be the case that *NUCB2* was induced by a low or undetectable level of ER in these cases. However, it is also true that estrogen-mediated induction of *NUCB2* mRNA was relatively slow in MCF-7 cells in our time-course study (Fig. 1C), suggesting that *NUCB2* expression is, at least in a part, induced by secondary responses, although the half-life of mRNA is an important factor in determining how long it takes to detect a change in the mRNA level of a specific gene.⁽⁴⁾ In addition, *NUCB2* is expressed in various human tissues not necessarily considered targets for estrogens, as described above.⁽²⁹⁾ Therefore, other factors than estrogens might be involved in the expression of *NUCB2* in breast carcinoma cells. No information is currently available regarding the regulation mechanisms of *NUCB2* expression to the best of our knowledge, and further research is required.

Previous studies have shown that ICI 182780 possesses a greater ability to suppress estrogen-sensitive gene expression and greater antitumor activity than tamoxifen in breast carcinoma.⁽³⁰⁾ This is partly due to the fact that ICI 182780 does not have agonistic ER activity and reduces steady-state levels of ER by increasing the turnover of the protein, whereas tamoxifen does possess partial agonistic ER activity.⁽³¹⁾ In our study, ICI 182780 was superior to tamoxifen in suppressing estradiol-mediated induction of *NUCB2* mRNA in MCF-7 cells (Fig. 1B), which is consistent with previous studies.

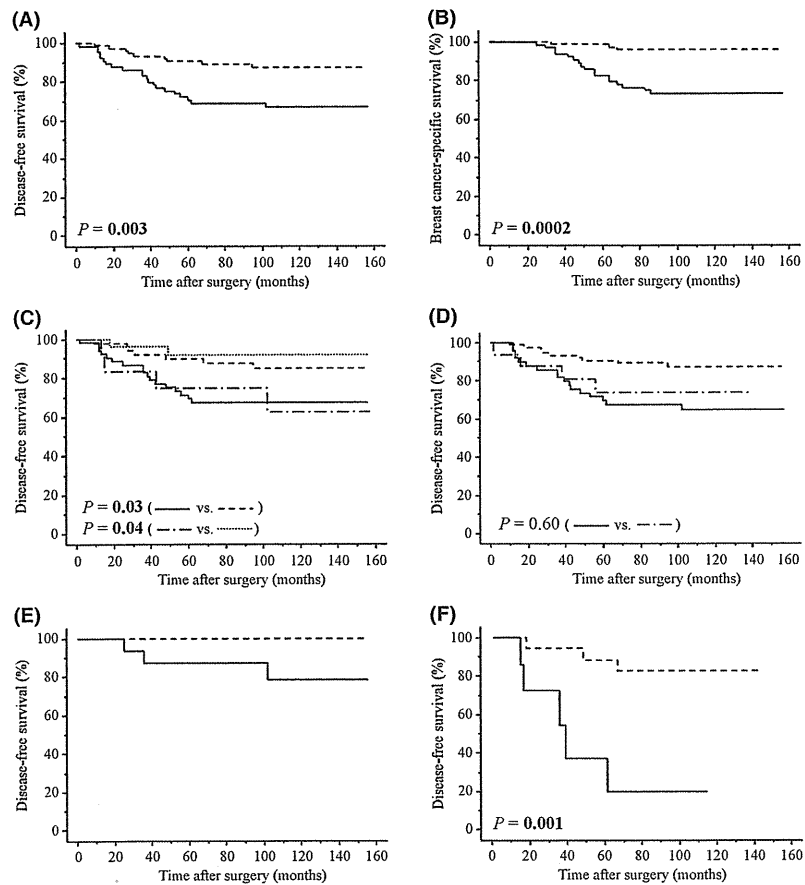


Fig. 3. Disease-free and breast cancer-specific survival of 141 breast carcinoma patients according to nucleobindin 2 (*NUCB2*) status. (A,B) *NUCB2* status was significantly associated with an increased risk of recurrence ($P = 0.003$) (A) and worse prognosis ($P = 0.0002$) (B). Solid line, positive for *NUCB2* ($n = 66$); dashed line, negative for *NUCB2* ($n = 75$). (C) Disease-free survival curve according to *NUCB2*/Ki-67 status. Solid line, positive for *NUCB2*/Ki-67 labeling index (LI) $\geq 10\%$ ($n = 54$); dashed line, positive for *NUCB2*/Ki-67 LI $< 10\%$ ($n = 12$); dotted line, negative for *NUCB2*/Ki-67 LI $\geq 10\%$ ($n = 50$); dot-dashed line, negative for *NUCB2*/Ki-67 LI $< 10\%$ ($n = 25$). (D) Disease-free survival curve according to *NUCB2* immunointensity. Solid line, strongly positive ($n = 16$); dashed line, modestly positive ($n = 50$); dot-dashed line, negative ($n = 75$). (E) *NUCB2* status was associated with recurrence in 40 patients who received tamoxifen therapy. P -value not available as there were no patients with recurrent disease in the *NUCB2*-negative group. Solid line, positive for *NUCB2* ($n = 16$); dashed line, negative for *NUCB2* ($n = 24$). (F) *NUCB2* status was significantly ($P = 0.001$) associated with recurrence in a group with estrogen receptor labeling index $< 1\%$ ($n = 24$). Solid line, positive for *NUCB2* ($n = 7$); dashed line, negative for *NUCB2* ($n = 17$).

In our present study, *NUCB2* immunoreactivity was positively associated with the presence of lymph node metastasis in breast carcinoma tissue both in ER-positive and ER-negative cases. In addition, subsequent *in vitro* studies indicated that both MCF-7 and SK-BR-3 cells transfected with siRNA *NUCB2* significantly decreased cell proliferation, and migration and invasion properties. Metastasis is considered as the major cause of treatment failure and death of carcinoma patients. It is a multistep process that involves migration and invasion of carcinoma cells, lymphogenous and/or hematogenous spread, and cell proliferation in the metastatic sites. Previous studies have shown that *NUCB2* has a wide variety of basic cellular functions, including an involvement in the energy homeostasis,⁽⁹⁾ Ca^{2+} homeostasis,⁽⁸⁾ and extracellular tumor necrosis factor receptor type 1 release,⁽¹⁰⁾ although the biological functions have not yet been fully clarified. Results of our present study suggest that *NUCB2* plays a pivotal role, especially in the metastasis of breast carcinomas, and serve as a starting point for clarification of the biological roles of *NUCB2* in breast carcinoma. However, we could not necessarily detect a significant association between *NUCB2* status and mitotic score, Ki-67 LI, or invasion status in the clini-

cal samples. Therefore, other factors might also play important roles in the processes of proliferation and invasion in breast carcinoma tissues.

In our present study, *NUCB2* status was also significantly associated with recurrence and worse prognosis in breast carcinoma patients, and a similar tendency was also detected in ER-positive patients who received tamoxifen therapy, or in ER-negative cases. In addition, results of multivariate analyses showed that *NUCB2* status was indeed an independent prognostic factor for both recurrence and breast cancer-specific survival. Results of our *in vitro* study indicated that tamoxifen inhibited estradiol-mediated induction of *NUCB2* expression in MCF-7 cells, but the basal expression level of *NUCB2* mRNA still remained. Considering that the *NUCB2* expression level was the highest among the genes predominantly expressed in the recurrence group despite tamoxifen therapy (group A in Fig. 1A), *NUCB2* status in breast carcinoma tissues at the time of surgery might reflect the basal level of *NUCB2* as well as the level induced by estrogens in breast carcinoma cases. Therefore, residual carcinoma cells following surgical treatment in *NUCB2*-positive breast carcinomas could still have the potential to rapidly grow and/or metastasize,

Table 2. Univariate and multivariate analyses of disease-free survival and breast cancer-specific survival in patients with stage I–III breast cancer (n = 141)

Variable	Univariate	Multivariate	
	P-value	P-value	Relative risk (95% CI)
Disease-free survival			
Lymph node metastasis (positive/negative)	<0.0001	0.0100	3.1 (1.3–7.6)
ER status (negative/positive)	0.0020	0.0020	4.8 (1.8–13.0)
<i>NUCB2</i> status (positive/negative)	0.0100	0.0010	4.6 (1.8–11.4)
<i>HER2</i> status (positive/negative)	0.0100	0.6600	ND
Tumor size (≥2.0 cm/<2.0 cm)	0.0200	0.1300	ND
Histological grade (3/1, 2)	0.0900	ND	ND
Ki-67 LI (≥10%/<10%)	0.3500	ND	ND
Menopausal status (pre/post)	0.6400	ND	ND
Breast cancer-specific survival			
Lymph node metastasis (positive/negative)	0.0004	0.2200	ND
<i>NUCB2</i> status (positive/negative)	0.0020	0.0004	12.0 (3.0–47.7)
ER status (negative/positive)	0.0030	0.0100	5.6 (1.5–20.7)
Histological grade (3/1,2)	0.0100	0.2800	ND
<i>HER2</i> status (positive/negative)	0.0100	0.6000	ND
Tumor size (≥2.0 cm/<2.0 cm)	0.0200	0.0700	ND
Ki-67 LI (≥10%/<10%)	0.1000	ND	ND
Menopausal status (post/pre)	0.7800	ND	ND

Data considered significant ($P < 0.05$) in the univariate analyses are shown in bold, and were examined in the multivariate analyses. CI, confidence interval; ER, estrogen receptor; LI, labeling index; ND, not done; *NUCB2*, nucleobindin 2; PR, progesterone receptor.

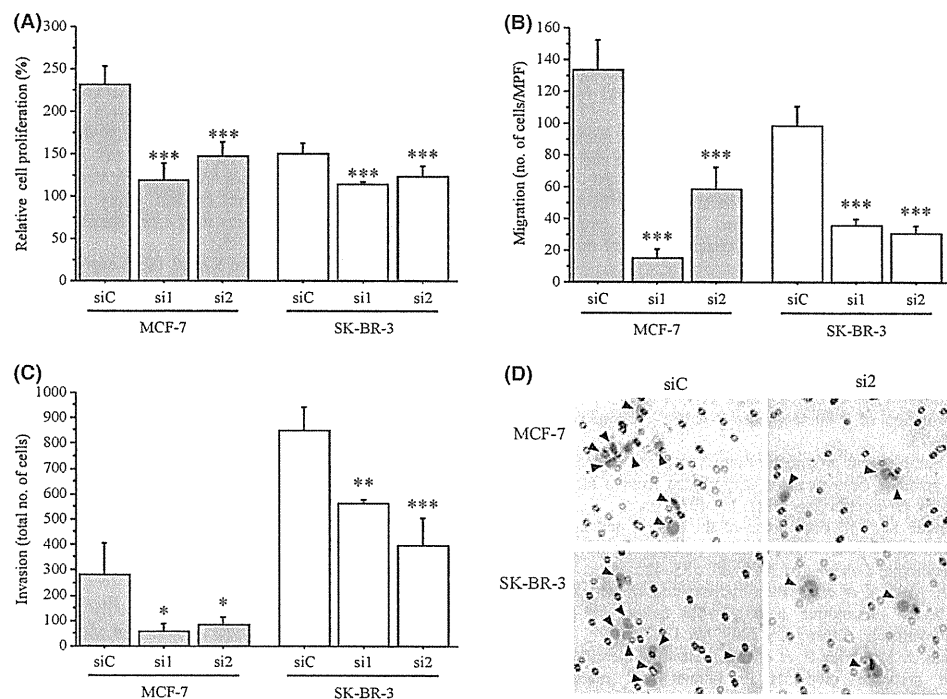


Fig. 4. Effects of nucleobindin 2 (*NUCB2*) on proliferation (A), and migration (B) and invasion (C,D) properties in breast carcinoma cells. (A–C) MCF-7 (gray bar) and SK-BR-3 (open bar) were transfected with *NUCB2*-specific siRNA (si1, si2) or control siRNA (siC). The relative cell proliferation was evaluated as a ratio (%) compared to that at 0 day after treatment (A). Migration ability was evaluated as an average number of cells in five middle power fields (MPF) ($\times 200$) on the lower surface of the membrane (B). Invasion ability was evaluated as the total number of cells (C). Data are presented as the mean \pm SD ($n = 6$ [A]; $n = 3$ [B,C]). * $P < 0.05$; ** $P < 0.01$; * $P < 0.001$ versus control cells (left bar). (D) Representative microphotographs of results of invasion assay. Invaded carcinoma cells (arrows) were observed with 8 μ m-sized pore. Nuclei stained with hematoxylin. When MCF-7 (upper panel) and SK-BR-3 (lower panel) cells were transfected with *NUCB2*-specific siRNA (si2) (right panel), the number of invading cells was decreased compared to the corresponding control (transfection with control siRNA [siC], left panel). Bar = 100 μ m.**

despite the fact that tamoxifen therapy partially suppresses the *NUCB2* expression level, thereby resulting in an increased recurrence and poor prognosis in these patients.

In summary, *NUCB2* was newly identified as a gene associated with recurrence in breast carcinoma patients by microarray analysis, and a subsequent *in vitro* study indicated that *NUCB2*

expression was upregulated by estrogen in MCF-7 cells. *NUCB2* immunoreactivity was detected in 48% of breast carcinoma tissues, and was an independent prognostic factor of the patients. Results of further *in vitro* studies showed that *NUCB2* significantly increased the proliferation activity, and migration and invasion properties both in MCF-7 and SK-BR-3 cells. These findings suggest that *NUCB2* plays an important role, especially in the metastasis of breast carcinoma, and *NUCB2* status in primary breast carcinoma is reasonably considered a potent prognostic factor.

Acknowledgments

We appreciate the skillful technical assistance of Mr. Katsuhiko Ono (Department of Anatomic Pathology, Tohoku University Graduate

School of Medicine, Sendai, Japan). This work was partly supported by a Grant-in-Aid for Scientific Research from the Japanese Ministry of Education, Culture, Sports, Science and Technology.

Disclosure Statement

The authors have no conflicts of interest.

Abbreviations

ER	estrogen receptor
ERE	estrogen-responsive element
LI	labeling index
NUCB2	nucleobindin 2
PR	progesterone receptor

References

- Jordan VC. Fourteenth Gaddum Memorial Lecture. A current view of tamoxifen for the treatment and prevention of breast cancer. *Br J Pharmacol* 1993; **110**: 507–17.
- Ali S, Coombes RC. Endocrine-responsive breast cancer and strategies for combating resistance. *Nat Rev Cancer* 2002; **2**: 101–12.
- Suzuki T, Inoue A, Miki Y *et al*. Early growth responsive gene 3 in human breast carcinoma: a regulator of estrogen-mediated invasion and a potent prognostic factor. *Endocr Relat Cancer* 2007; **14**: 279–92.
- Frasor J, Danes JM, Komm B, Chang KC, Lytle CR, Katzenellenbogen BS. Profiling of estrogen up- and down-regulated gene expression in human breast cancer cells: insights into gene networks and pathways underlying estrogenic control of proliferation and cell phenotype. *Endocrinology* 2003; **144**: 4562–74.
- Hayashi SI, Eguchi H, Tanimoto K *et al*. The expression and function of estrogen receptor alpha and beta in human breast cancer and its clinical application. *Endocr Relat Cancer* 2003; **10**: 193–202.
- Miura K, Titani K, Kurosawa Y, Kanai Y. Molecular cloning of nucleobindin, a novel DNA-binding protein that contains both a signal peptide and a leucine zipper structure. *Biochem Biophys Res Commun* 1992; **187**: 375–80.
- Barnikol-Watanabe S, Gross NA, Götz H *et al*. Human protein NEFA, a novel DNA binding/EF-hand/leucine zipper protein. Molecular cloning and sequence analysis of the cDNA, isolation and characterization of the protein. *Biol Chem Hoppe Seyler* 1994; **375**: 497–512.
- Taniguchi N, Taniura H, Niinobe M *et al*. The postmitotic growth suppressor necdin interacts with a calcium-binding protein (NEFA) in neuronal cytoplasm. *J Biol Chem* 2000; **275**: 31674–81.
- Oh IS, Shimizu H, Satoh T *et al*. Identification of nesfatin-1 as a satiety molecule in the hypothalamus. *Nature* 2006; **443**: 709–12.
- Islam A, Adami B, Hawari FI *et al*. Extracellular TNFR1 release requires the calcium-dependent formation of a nucleobindin 2-ARTS-1 complex. *J Biol Chem* 2006; **281**: 6860–73.
- Elston CW, Ellis IO. Pathological prognostic factors in breast-cancer. 1. The value of histological grade in breast-cancer -experience from a large study with long-term follow-up. *Histopathology* 1991; **19**: 403–10.
- Miki Y, Suzuki T, Kitada K *et al*. Expression of the steroid and xenobiotic receptor and its possible target gene, organic anion transporting polypeptide-A, in human breast carcinoma. *Cancer Res* 2006; **66**: 535–42.
- Nagasaki S, Suzuki T, Miki Y *et al*. 17Beta-hydroxysteroid dehydrogenase type 12 in human breast carcinoma: a prognostic factor via potential regulation of fatty acid synthesis. *Cancer Res* 2009; **69**: 1392–9.
- Bourdeau V, Deschênes J, Me'tivier R *et al*. Genomewide identification of high-affinity estrogen response elements in human and mouse. *Mol Endocrinol* 2004; **18**: 1411–27.
- Kalnina Z, Silina K, Bruvere R *et al*. Molecular characterisation and expression analysis of SEREX-defined antigen NUCB2 in gastric epithelium, gastritis and gastric cancer. *Eur J Histochem* 2009; **53**: 7–18.
- Takagi K, Miki Y, Nagasaki S *et al*. Increased intratumoral androgens in human breast carcinoma following aromatase inhibitor exemestane treatment. *Endocr Relat Cancer* 2010; **17**: 415–30.
- Oka K, Suzuki T, Onodera Y *et al*. Nudix-type motif 2 in human breast carcinoma: a potent prognostic factor associated with cell proliferation. *Int J Cancer* 2011; **128**: 1770–82.
- Ramanjaneya M, Chen J, Brown JE *et al*. Identification of nesfatin-1 in human and murine adipose tissue: a novel depot-specific adipokine with increased levels in obesity. *Endocrinology* 2010; **151**: 3169–80.
- Oh DS, Troester MA, Usary J *et al*. Estrogen-regulated genes predict survival in hormone receptor-positive breast cancers. *J Clin Oncol* 2006; **24**: 1656–64.
- Huang E, Cheng SH, Dressman H *et al*. Gene expression predictors of breast cancer outcomes. *Lancet* 2003; **361**: 1590–6.
- Naoi Y, Kishi K, Tanei T *et al*. Development of 95-gene classifier as a powerful predictor of recurrences in node-negative and ER-positive breast cancer patients. *Breast Cancer Res Treat* 2011; **128**: 633–41.
- van't Veer LJ, Dai H, van de Vijver MJ *et al*. Gene expression profiling predicts clinical outcome of breast cancer. *Nature* 2002; **415**: 530–6.
- Paik S. Development and clinical utility of a 21-gene recurrence score prognostic assay in patients with early breast cancer treated with tamoxifen. *Oncologist* 2007; **12**: 631–5.
- Sotiriou C, Wirapati P, Loi S *et al*. Gene expression profiling in breast cancer: understanding the molecular basis of histologic grade to improve prognosis. *J Natl Cancer Inst* 2006; **98**: 262–72.
- Hao X, Sun B, Hu L *et al*. Differential gene and protein expression in primary breast malignancies and their lymph node metastases as revealed by combined cDNA microarray and tissue microarray analysis. *Cancer* 2004; **100**: 1110–22.
- Li X, Cao X, Li X, Zhang W, Feng Y. Expression level of insulin-like growth factor binding protein 5 mRNA is a prognostic factor for breast cancer. *Cancer Sci* 2007; **98**: 1592–6.
- Booth BW, Smith GH. Roles of transforming growth factor-alpha in mammary development and disease. *Growth Factors* 2007; **25**: 227–35.
- Klebig C, Korinth D, Meraldi P. Bub1 regulates chromosome segregation in a kinetochore-independent manner. *J Cell Biol* 2009; **185**: 841–58.
- García-Galiano D, Navarro VM, Gaytan F, Tena-Sempere M. Expanding roles of NUCB2/nesfatin-1 in neuroendocrine regulation. *J Mol Endocrinol* 2010; **45**: 281–90.
- Osborne CK, Coronado-Heinsohn EB, Hilsenbeck SG *et al*. Comparison of the effects of a pure steroidal antiestrogen with those of tamoxifen in a model of human breast cancer. *J Natl Cancer Inst* 1995; **87**: 746–50.
- Dauvois S, White R, Parker MG. The antiestrogen ICI 182780 disrupts estrogen receptor nucleocytoplasmic shuttling. *J Cell Sci* 1993; **106**: 1377–88.

Supporting Information

Additional Supporting Information may be found in the online version of this article:

Table S1. Genes predominantly expressed in the non-recurrence group, classified as group B.

Table S2. Association between nucleobindin 2 (*NUCB2*) status and clinicopathological parameters according to estrogen receptor status in 161 breast carcinomas.

Please note: Wiley-Blackwell are not responsible for the content or functionality of any supporting materials supplied by the authors. Any queries (other than missing material) should be directed to the corresponding author for the article.

Melatonin suppresses aromatase expression and activity in breast cancer associated fibroblasts

Kevin C. Knowler · Sarah Q. To · Kiyoshi Takagi ·
Yasuhiro Miki · Hironobu Sasano · Evan R. Simpson ·
Colin D. Clyne

Received: 7 December 2011 / Accepted: 4 January 2012 / Published online: 12 January 2012
© Springer Science+Business Media, LLC. 2012

Abstract The main biological active substance secreted by the pineal gland, melatonin (MLT), counteracts the effects of estrogens in breast cancer via exerting a number of its own oncostatic properties. Recent studies of postmenopausal women have identified that the major metabolite of MLT is statistically significantly associated with a lower risk of developing breast cancer. While MLT production decreases with age, breast cancer risk, however, increases with age and obesity. We hypothesize that MLT inhibits estrogen production in breast adipose fibroblasts (BAFs), the main local source of estrogen in breast tumors of postmenopausal women, by inhibiting transcription of the *CYP19A1* gene that encodes the key enzyme aromatase. Normal BAFs were cultured from women undergoing breast reduction surgery, while breast cancer-associated fibroblasts (CAFs) were isolated from three women with estrogen receptor (ER) positive invasive ductal carcinomas. *MTNR1A* and *MTNR1B* receptor expression and *CYP19A1* mRNA expression following MLT treatments were determined by qRT-PCR.

BAFs express the G-protein coupled MLT receptors *MTNR1A* and *MTNR1B* with elevated levels of *MTNR1A* found in CAFs. Treatment of BAFs and CAFs with MLT resulted in significant suppression of *CYP19A1* transcription and aromatase activity at pharmacological, physiological and sub-physiological concentrations. MLT suppression occurred through promoter-specific PI.4-, PI.3- and PII-derived *CYP19A1* mRNA. Stimulation of *CYP19A1* PII-mRNA and aromatase activity by prostaglandin E₂ (PGE₂) were significantly attenuated by physiological doses of MLT. Lower levels of MLT in aging women may increase the risk of progressing ER-positive breast cancer through a decreased ability to suppress *CYP19A1* expression and subsequent local estrogen production in BAFs/CAFs.

Keywords Melatonin · Aromatase · Postmenopause · Breast cancer · Epigenetic · Prostaglandin E₂

Introduction

Breast cancer is a classical model of hormone-dependent malignancy. Two-thirds of breast cancer occurs in postmenopausal women, where ovaries have ceased to be functional and changes in the hormonal milieu are associated with an increase in total adiposity and breast cancer risk. Aromatase P450, encoded by the gene *CYP19A1*, is the key enzyme catalysing the synthesis of estrogens from circulating C₁₉ steroids [1]. In postmenopausal women, cancer-associated fibroblasts (CAFs, also referred to as breast adipose fibroblasts (BAFs) in the absence of a tumor) of the stromal compartment adjacent to a tumor become the major source of local estrogen production, coinciding with an increase in *CYP19A1* expression via the tissue-specific promoters PI.4, PI.3 and PII in these cells

K. C. Knowler (✉) · S. Q. To · C. D. Clyne
Cancer Drug Discovery Laboratory, Prince Henry's Institute
of Medical Research, P.O. Box 5152, Clayton, VIC 3168,
Australia
e-mail: kevin.knowler@princehenrys.org

K. Takagi · Y. Miki · H. Sasano
Department of Pathology, Tohoku University Graduate
School of Medicine, Sendai, Japan

E. R. Simpson
Metabolism and Cancer Laboratory, Prince Henry's Institute,
Clayton, VIC, Australia

E. R. Simpson · C. D. Clyne
Department of Biochemistry and Molecular Biology, Monash
University, Clayton, VIC, Australia

[2]. The stimulation of these tissue-specific promoters occurs through paracrine signals, such as prostaglandin E₂ (PGE₂) (PI.3/II) and class I cytokines and glucocorticoids (PI.4), derived from neighboring tumor epithelial cells and infiltrating macrophages [3, 4]. The development of breast-specific aromatase inhibitors (AIs) and suppressors of *CYP19A1* gene expression is therefore a critical aspect in inhibiting local estrogen production in breast cancer and is at the frontline of therapeutic care.

The main biological active substance secreted by the pineal gland, melatonin (MLT), can counteract the effects of estrogens in breast cancer through a number of its own oncostatic properties and signaling mechanisms [5–7]. MLT hormone is secreted in response to darkness and, as such, levels rise and fall throughout the day. Evidence from clinical studies has led to the hypothesis that increased risk for breast cancer among women is closely related to circulating MLT levels. For example, light-induced inhibition of MLT secretion increases breast cancer risks, e.g. within flight attendants and night-shift workers; conversely, totally blind women also have the lowest incidence of breast cancer [8]. A recent cohort study of postmenopausal women has also revealed that an increased concentration of urinary 6-sulfatoxymelatonin (aMT6s), the major metabolite of MLT, is statistically significantly associated with a lower risk of developing breast cancer [9]. These observations are further supported by the fact that MLT production gradually declines with advancing age, with MLT levels reported to be low in elderly individuals, associated with ER-positive breast cancer and linked with enhanced tumor growth in rats [10–12].

Since surrounding BAFs are the major source of local estrogen production in postmenopausal women, it is possible that many of the protective properties of MLT are exerted upon these cells but lost with increasing age. Physiological concentrations of MLT have been shown to reduce aromatase expression and activity in the ER-positive breast cancer derived cell line MCF-7 [13, 14]. However, it is acknowledged that CAFs, not epithelial cells, are the abundant source of elevated *CYP19A1* mRNA in postmenopausal breast cancer [15]. In this study we show that MLT suppresses *CYP19A1* mRNA expression and aromatase activity in normal BAFs and CAFs obtained from women with ER-positive invasive ductal carcinoma (IDC).

Materials and methods

Patient information

Subcutaneous adipose tissue was obtained from Caucasian cancer-free women at the time of reduction mammoplasty approved by the Southern Health Human Ethics Research

Committee at Prince Henry's Institute. Specimens of IDC of the breast were obtained from Japanese female patients at Tohoku University Hospital and Tohoku Kosai Hospital. Relevant clinical data were retrieved from the review of the patients' files. The histologic grade of each specimen was independently evaluated. The ethics committees at Tohoku University School of Medicine and Tohoku Kosai Hospital approved the research protocols (2004-144, 2005-068, and 2006-042, respectively), with informed consent being obtained from these patients before surgery in each institution.

Cell culture

Human breast adipose fibroblasts were isolated by collagenase digestion and cultured as previously described [16]. Where BAFs were used as a comparison to other cell types, averaged data were obtained from BAFs isolated from three independent women. Cell line MCF-7 (ATCC No. HTB-22) was subcultured according to supplier's procedures. For treatments, BAFs grown to ~60% confluence were initially starved in serum-free media containing 0.1% BSA for 24 h. MLT was prepared in dimethyl sulfoxide (DMSO) at described concentrations and cells were treated in serum-free media for 90 min. To stimulate promoter-specific *CYP19A1* transcription, serum-free media containing PGE₂ (1 μM) was added to cells for 24 h to stimulate PII. In all treatments, equal amounts of vehicle alone (the agent in which the compound was dissolved) were used as a control.

RNA isolation and quantitative RT-PCR

Total RNA was isolated from cells using the RNeasy Mini kit (QIAGEN). Following DNase treatment, first strand cDNA synthesis from a minimum of 200 ng of total RNA was performed using AMVRT (Promega) primed by random hexamers. Semi-quantitative RT-PCR of *MTNRIA* and *MTNR1B* receptors was performed with the primer pairs for *MTNRIA*—(Fwd) 5'-GCCACAGTCTCAAGTACGACA-3' (Rev) 5'-CTGGAGAACCAGGATCCATAT-3' and *MTNR1B*—(Fwd) 5'-TGCCTCATCTGGCTCCTCAC-3' (Rev) 5'-TAGGGAGGAGGAAGTGGATG-3'. Quantitative RT-PCR (qRT-PCR) of total *CYP19A1* mRNA was performed with SYBR Green detection methodologies with Roche LightCycler Systems using the primer pair termed RT-7 (Fwd) 5'-TTGGAAATGCTGAACCCGAT-3' and RT-8 (Rev) 5'-CAGGAATCTGCCGTGGGGAT-3'; or the ABI 7900HT Sequence Detection System using (Fwd) 5'-CACATCCTCAATACCAGGTCC-3' and (Rev) 5'-CAGAGATCCAGACTCGCATG-3' and probe 5'-6-FAM-CCCTCATCTCCCACGGCAGATTCC-TAMRA-3'. PII-driven transcripts were quantitated with Roche LightCycler

using (Fwd) 5'-GCAACAGGAGCTATAGAT-3' and RT-8; or the ABI 7900HT using (Fwd) 5'-GCAACAGGAGCTATAGATGAA-3' and ExonII (Rev) 5'-AGGCACGATGCTGGTGATG-3' and probe 5'-6-FAM-TGCCCCCTCTGAGGTCAAGGAACA-TAMRA-3'. In combination with ExonII (Rev)-PI.4 (Fwd) 5'-GTAGAACGTGACCAAC TGGAG-3' and probe 5'-6-FAM-ATGGGCTGACCAGTGCCAGGGACC-TAMRA-3'; PI.3 (Fwd) 5'-GTCTTGCC TAAATGTCTGATCAC-3' and probe 5'-6-FAM-TGCCCC CTCTGAGGTCAAGGAACAC-TAMRA-3' were quantitated with the ABI 7900HT. qRT-PCR amplification of *18S* was conducted with SYBR Green detection methodologies using (Fwd) 5'-CGGCTACCACATCCAAGGA-3' and (Rev) 5'-GCTGGAATTACCGCGGCT-3'.

Aromatase activity assays

BAFs and CAFs were grown to ~60% confluence and then serum starved overnight in phenol-red free medium containing 0.1% BSA. After serum starvation, cells were treated with experimental agents at the concentrations indicated for 24 h. Endogenous aromatase activity was measured by the detection of 3HOH released during aromatization of [1 β -3H] androstenedione, as previously described [16].

Statistical analysis

Data were analyzed by one-way ANOVA followed by Newman-Keuls Multiple Comparison test. Statistical analysis was performed with GraphPad Prism Software.

Results

MLT acts through its G-protein-coupled receptors, MT1 and MT2, located at the plasma membrane. Initially, expression of encoding genes *MTNRIA* (MT1) and *MTNRIB* (MT2) was assessed in BAFs by qRT-PCR. BAFs and MCF-7 (positive control) cells expressed both receptors, albeit to differing levels, with *MTNRIA* levels predominantly lower in BAFs compared to MCF-7 cells (Fig. 1a). Following confirmation of MLT receptor expression, to determine whether MLT altered *CYP19A1* mRNA expression, pharmacological (10 μ M), physiological (1 nM) and sub-physiological (10 pM) concentrations of MLT were used to treat BAFs. In each instance, a significant suppression of total *CYP19A1* mRNA levels was observed when compared to vehicle alone (100%); 51% (10 pM), 28% (1 nM), and 35% (10 μ M) (Fig. 1b). Following the observed suppression of *CYP19A1* mRNA, aromatase activity assays were performed to measure the

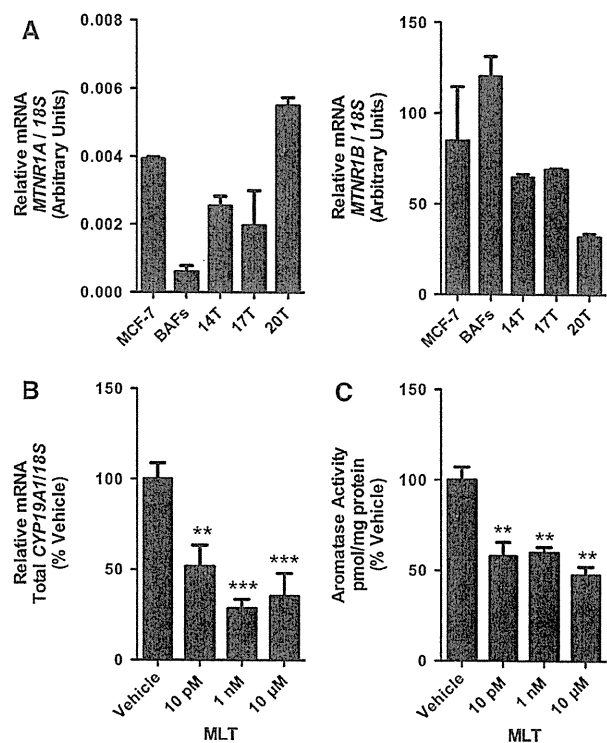


Fig. 1 MLT suppresses *CYP19A1* mRNA expression and activity in BAFs. **a** qRT-PCR of *MTNRIA* and *MTNRIB* in cDNA from BAFs and MCF-7 cells. cDNA from primary CAF lines 14T, 17T and 20T (Table 1) were also analyzed. **b** qRT-PCR of total *CYP19A1* mRNA in BAFs treated with final concentrations of 10 pM, 1 nM and 10 μ M of MLT for 90 min. **c** Aromatase activity in BAFs following 24 h treatments of MLT. Data obtained from two to three independent experiments. Error bars represent standard error of means. Data was analyzed by one-way ANOVA followed by Newman-Keuls multiple comparison test (** $p < 0.01$, *** $p < 0.001$)

production of estrogen by measuring the transfer of tritium at the 1 β position of [1 β -3H]androstenedione (1 β -AE) to water. In comparison to vehicle alone (100%), significant decreases in aromatase activity were observed in BAFs treated with MLT—57% (10 pM), 60% (1 nM) and 48% (10 μ M) (Fig. 1c).

Expression of *CYP19A1* in BAFs is under the control of the tissue-specific promoters PI.4, PI.3 and PII, with PI.4 being the predominant transcript present in disease-free cells. To ascertain if the effects of MLT is promoter specific, exon-specific qRT-PCR was performed for each promoter following MLT treatment. Physiological concentrations of MLT (1 nM) significantly decreased expression of all three promoters when compared to vehicle (100%); PI.4 (34%), PI.3 (48%) and PII (42%) (Fig. 2a). The secretion of PGE₂ by breast tumor epithelial cells is associated with the increased tumor PII-derived transcriptional activity in surrounding BAFs through both cAMP/PKA- and PKC-dependent signaling and the

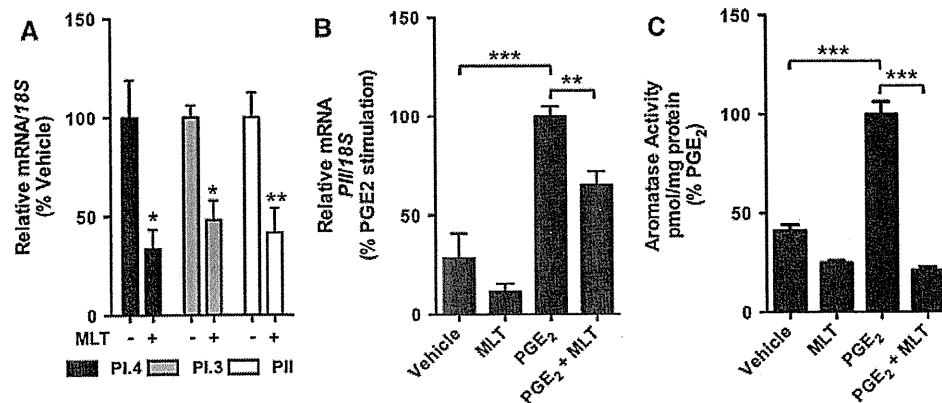


Fig. 2 Suppressive effects of MLT on promoter-specific *CYP19A1* expression and activity in BAFs. **a** Exon-specific qRT-PCR of *CYP19A1* promoters PI.4, PI.3 and PII following MLT (1 nM) treatment. **b** Exon-specific qRT-PCR of PII-derived mRNA following PGE₂ (1 μM) stimulation alone or in combination with MLT (1 nM).

c Aromatase activity following PGE₂ (1 μM) stimulation alone or in combination with MLT (1 nM). Data obtained from three independent experiments. Error bars represent standard error of means. Data was analyzed by one-way ANOVA followed by Newman–Keuls multiple comparison test (* $p < 0.05$, ** $p < 0.01$, *** $p < 0.001$)

activation of a number of transcription factors [3]. As MLT is known to decrease intracellular concentrations of cAMP [14], we tested the ability of MLT to suppress PGE₂ PII-stimulation in BAFs. PGE₂ increased PII-derived *CYP19A1* mRNA ~3.5-fold compared to vehicle (Fig. 2b). In the presence of physiological concentrations of MLT, however, the PII-stimulation was significantly decreased (65%) compared to PGE₂ alone treatment (100%) (Fig. 2b). Likewise, PGE₂ stimulated aromatase activity ~2-fold, a process that is also significantly reduced following co-treatment with MLT (21%) (Fig. 2c).

As MLT was found to suppress *CYP19A1* expression in BAFs isolated from normal women, we extended these observations to CAFs isolated from women with ER-positive IDC (Table 1). Three tumor primary cell lines, two from postmenopausal women (Patient ID: 17T and 20T) and one from premenopausal (Patient ID: 14T) were initially screened for aromatase activity levels. The three CAF lines showed significant higher levels of aromatase activity, upwards of ~2-fold in the case of 14T and 20T, compared to disease-free BAFs (Fig. 3). *MTNR1A* and *MTNR1B* receptor expression was determined by qRT-PCR. All three CAF lines maintained MLT receptor expression; however, our findings demonstrated higher levels of *MTNR1A* and lower levels of *MTNR1B* mRNA in the three CAF lines compared to disease-free BAFs (Fig. 1a). Physiological doses of MLT were used to treat CAFs and total *CYP19A1* mRNA levels and aromatase activity assessed. When compared to vehicle alone treatments (100%), each CAF had significantly reduced levels of total *CYP19A1* mRNA following MLT treatment; 14T (37%), 17T (29%) and 20T (43%) (Fig. 4a). This reduction also conferred into a significant decrease in aromatase activity compared to vehicle (100%); 14T (22%), 17T (41%) and 20T (37%).

Discussion

Multiple lines of in vivo and in vitro evidence show that the MLT oncostatic actions in breast cancer are primarily through its effects on hormone-dependent tumors through its ability to interact with estrogen signaling pathways [5]. In tumor epithelial cells, these interactions have shown to modulate estrogen receptor actions as well as the enzymes responsible for estrogen biosynthesis [17]. Crosstalk within the IDC breast tumor microenvironment results in the elevated levels of aromatase expression in neighboring adipose fibroblasts and the main source of local estrogen in postmenopausal women. In this study we demonstrate MLT oncostatic actions on normal BAFs and CAFs isolated from IDCs, two of which were postmenopausal, to down-regulate aromatase mRNA expression at physiological concentrations. Both BAFs and CAFs predominately express the *MTNR1A* receptor, which may correlate to the binding of MLT to MT1 as seen as one of the first steps in aromatase antagonism in epithelial cells [18].

Understanding the promoter-specific control of *CYP19A1* expression in BAFs is fundamental for creating modes of antagonism. While PI.4 is elevated in the presence of a tumor, PI.3 and PII make up 80–90% of *CYP19A1*-derived transcripts also up-regulated, as such, much work has been carried out to understand this regulatory pathway as a means to decrease aromatase expression [19]. In this study, we show that MLT actions on BAFs are not promoter-specific and suppress each of the three promoters expressed. This data correlates with what is observed in MCF-7 cells despite the subtle differences in modes of PII transcriptional activation by alternative transcription factors in the two different cell types [14, 20]. Elevated levels of PI.4 in CAFs are due to elevated levels of class I cytokines and glucocorticoids within the tumor

Table 1 The clinicopathological information of the three cases of breast cancer in which stromal cells were obtained

Sample ID	Age	Sex	Histopathological diagnosis	Nottingham's histological grade (tubular formation, nuclear atypia, mitosis)	TNM	ER	PgR	HER2
14T	47	F	Invasive ductal carcinoma, scirrhous carcinoma	Grade II (3, 2, 1)	pT1c, pN0, cM0, G2, Stage I	Positive (PS5 + IS3 = TS8, almost 100%)	Positive (PS5 + IS3 = TS8, almost 100%)	Negative (score 0)
17T	76	F	Invasive ductal carcinoma, scirrhous carcinoma	Grade II (3, 2, 1)	pT4b, pN1, cM0, G2, Stage IIIB	Positive (PS5 + IS3 = TS8, 100%)	Positive (PS4 + IS3 = TS7, 40%)	Negative (score 0)
20T	69	F	Invasive ductal carcinoma, scirrhous carcinoma	Grade II (2, 3, 1)	pT4b, pN0, cM0, G1, Stage IIIB	Positive (PS5 + IS3 = TS8, almost 100%)	Positive (PS5 + IS3 = TS8, almost 100%)	Negative (score 0)

Histological grade was determined according to Robbins et al. [28] and each score represents that of tubular formation, nuclear atypia and mitosis. ER and PR immunoreactivity was evaluated according to Allred et al. [29]. HER2 immunoreactivity was evaluated based on the CAP-ASCO guideline [30] PS proportional score, IS intensity score, TS total score

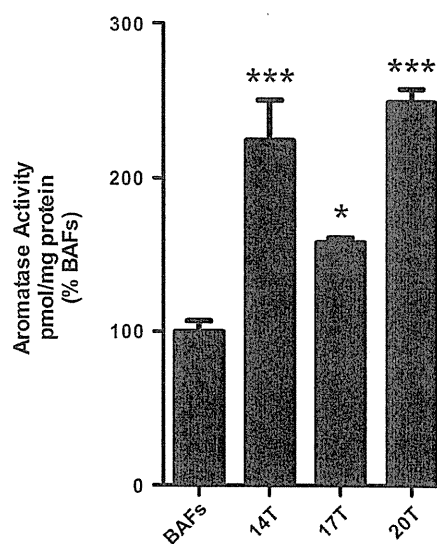


Fig. 3 Aromatase activity is elevated in 14T, 17T and 20T CAF lines. Data obtained from triplicate experiments. Error bars represent standard error of means. Data was analyzed by one-way ANOVA followed by Newman-Keuls multiple comparison test (* $p < 0.05$, *** $p < 0.001$)

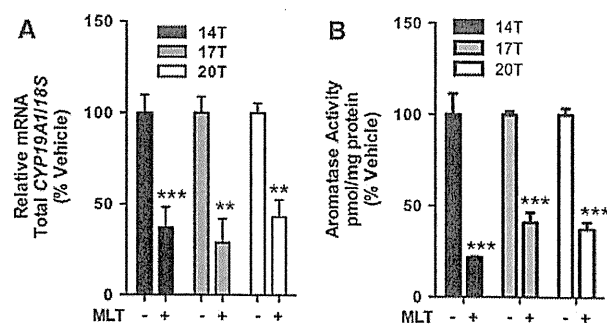


Fig. 4 MLT suppresses aromatase expression and activity in CAFs. **a** qRT-PCR of total *CYP19A1* mRNA from 14T, 17T and 20T CAF cell lines treated with MLT (1 nM) for 90 min. **b** Aromatase activity following 24-h treatment with MLT (1 nM). Data obtained from three experiments. Error bars represent standard error of means. Data was analyzed by one-way ANOVA followed by Newman-Keuls multiple comparison test (** $p < 0.01$, *** $p < 0.001$)

microenvironment. Interestingly, MLT can repress dexamethasone induced transcriptional activation in MCF-7 cells and reduce proinflammatory cytokines such as TNF- α and IL-6 [21, 22]. Factors such as these are critical for PI.4-driven *CYP19A1* expression and may serve as two possible modes of MLT PI.4 inhibition in BAFs.

The dramatic elevation of PI.3/PII transcripts in CAFs is a direct consequence of increases in cellular cAMP levels through PGE₂ secreted by tumor epithelial cells. By modeling this in BAFs, we show that this PII-driven stimulation by PGE₂ can be inhibited by MLT. Our data are consistent with previous observations that MLT can down-regulate

cAMP levels and downstream targets in different cell types including MCF-7 cells [14]. While elevated PGE₂ in the microenvironment, driven by increases in *COX-2* expression in tumor epithelial cells, acts on CAFs predominantly in a paracrine manner, up-regulation of *COX-2* in the stroma may also serve as a mechanism of PGE₂ autocrine action to stimulate PII. However, whereas MLT was shown to down-regulate *COX-2* expression in MCF-7 cells [14], our observations suggest that this is not the case in CAFs (data not shown).

The breast is delicately sensitive to interactions within the tumor microenvironment and has thus emerged as an important therapeutic target, with anti-stromal therapies now being added to the armament of anti-cancer weapons. The ability of MLT to suppress aromatase expression in multiple cell types within the breast tumor microenvironment, including CAFs as shown in this study, adds to the growing evidence supporting this non-toxic hormone to be used in the treatment of postmenopausal estrogen-dependent breast cancer. Not only can MLT disrupt the phenotype of aromatase expressing mouse fibroblasts [23], the suppressive effects of MLT on aromatase activity can also be enhanced when used in combination with the AI aminoglutethimide in vitro [24] and in vivo studies [25]. Furthermore, in combination with metformin, an AMPK-activator that inhibits aromatase expression in BAFs [26], MLT has shown to suppress mammary tumor growth in HER-2/neu transgenic mice [27]. The potential of metformin and melatonin used together to inhibit aromatase expression in the breast is yet to be tested and warrants further investigation.

In summary, our findings demonstrate a negative effect of MLT on aromatase expression in CAFs and reinforces the importance that circulating MLT levels may have in the protection against ER-receptor positive breast cancer.

Acknowledgments KCK was supported by a U.S. Department of Defense Post-doctoral Training Award (W81XWH-08-BCRP-POSTDOC). This work was supported by the National Health and Medical Research Council of Australia through fellowships to CDC (#338518) and ERS (#550900); the Victoria Breast Cancer Research Consortium Inc.; and the Victorian Government's Operational Infrastructure Support Program. PHI Data Audit #11-17.

Conflict of interest The authors declare that they have no conflicts of interest.

References

- Corbin CJ, Graham-Lorence S, McPhaul M, Mason JJ, Mendelson CR, Simpson ER (1988) Isolation of a full-length cDNA insert encoding human aromatase system cytochrome P-450 and its expression in nonsteroidogenic cells. *Proc Natl Acad Sci USA* 85(23):8948–8952
- Bulun SE, Price TM, Aitken J, Mahendroo MS, Simpson ER (1993) A link between breast cancer and local estrogen biosynthesis suggested by quantification of breast adipose tissue aromatase cytochrome P450 transcripts using competitive polymerase chain reaction after reverse transcription. *J Clin Endocrinol Metab* 77(6):1622–1628
- Zhao Y, Agarwal VR, Mendelson CR, Simpson ER (1996) Estrogen biosynthesis proximal to a breast tumor is stimulated by PGE₂ via cyclic AMP, leading to activation of promoter II of the CYP19 (aromatase) gene. *Endocrinology* 137(12):5739–5742
- Zhao Y, Nichols JE, Valdez R, Mendelson CR, Simpson ER (1996) Tumor necrosis factor- α stimulates aromatase gene expression in human adipose stromal cells through use of an activating protein-1 binding site upstream of promoter 1.4. *Mol Endocrinol* 10(11):1350–1357
- Grant SG, Melan MA, Latimer JJ, Witt-Enderby PA (2009) Melatonin and breast cancer: cellular mechanisms, clinical studies and future perspectives. *Expert Rev Mol Med* 11:e5
- Blask DE, Hill SM, Dauchy RT, Xiang S, Yuan L, Duplessis T, Mao L, Dauchy E et al (2011) Circadian regulation of molecular, dietary, and metabolic signaling mechanisms of human breast cancer growth by the nocturnal melatonin signal and the consequences of its disruption by light at night. *J Pineal Res* 51(3):259–269
- Mediavilla MD, Sanchez-Barcelo EJ, Tan DX, Manchester L, Reiter RJ (2010) Basic mechanisms involved in the anti-cancer effects of melatonin. *Curr Med Chem* 17(36):4462–4481
- Anisimov VN (2002) The light–dark regimen and cancer development. *Neuro Endocrinol Lett* 23(Suppl 2):28–36
- Schernhammer ES, Hankinson SE (2009) Urinary melatonin levels and postmenopausal breast cancer risk in the Nurses' Health Study cohort. *Cancer Epidemiol Biomarkers Prev* 18(1):74–79
- Iguichi H, Kato KI, Ibayashi H (1982) Age-dependent reduction in serum melatonin concentrations in healthy human subjects. *J Clin Endocrinol Metab* 55(1):27–29
- Tamarkin L, Danforth D, Lichter A, DeMoss E, Cohen M, Chabner B, Lippman M (1982) Decreased nocturnal plasma melatonin peak in patients with estrogen receptor positive breast cancer. *Science* 216(4549):1003–1005
- Hill SM, Cheng C, Yuan L, Mao L, Jockers R, Dauchy B, Frasch T, Blask DE (2011) Declining melatonin levels and MT1 receptor expression in aging rats is associated with enhanced mammary tumor growth and decreased sensitivity to melatonin. *Breast Cancer Res Treat* 127(1):91–98
- Cos S, Martinez-Campa C, Mediavilla MD, Sanchez-Barcelo EJ (2005) Melatonin modulates aromatase activity in MCF-7 human breast cancer cells. *J Pineal Res* 38(2):136–142
- Martinez-Campa C, Gonzalez A, Mediavilla MD, Alonso-Gonzalez C, Alvarez-Garcia V, Sanchez-Barcelo EJ, Cos S (2009) Melatonin inhibits aromatase promoter expression by regulating cyclooxygenases expression and activity in breast cancer cells. *Br J Cancer* 101(9):1613–1619
- Shibuya R, Suzuki T, Miki Y, Yoshida K, Moriya T, Ono K, Akahira J, Ishida T et al (2008) Intratumoral concentration of sex steroids and expression of sex steroid-producing enzymes in ductal carcinoma in situ of human breast. *Endocr Relat Cancer* 15(1):113–124
- Ackerman GE, Smith ME, Mendelson CR, MacDonald PC, Simpson ER (1981) Aromatization of androstenedione by human adipose tissue stromal cells in monolayer culture. *J Clin Endocrinol Metab* 53(2):412–417
- Gonzalez A, Cos S, Martinez-Campa C, Alonso-Gonzalez C, Sanchez-Mateos S, Mediavilla MD, Sanchez-Barcelo EJ (2008) Selective estrogen enzyme modulator actions of melatonin in human breast cancer cells. *J Pineal Res* 45(1):86–92
- Gonzalez A, Martinez-Campa C, Mediavilla MD, Alonso-Gonzalez C, Sanchez-Mateos S, Hill SM, Sanchez-Barcelo EJ,